

Review of the gas centrifuge until 1962. Part II: Principles of high-speed rotation

Stanley Whitley

British Nuclear Fuels Limited, Capenhurst Works, Chester, England

The principles of the separation physics of the gas centrifuge were described in Part I of this review. In this second section the principles involved in spinning the rotors of these centrifuges are described. Three types of rotor can be identified, depending on the ratio of length to diameter. If the rotor is very short, length-diameter ratio less than one, it is gyroscopically stable and easy to spin. If the length-diameter ratio is in the region of 4 or 5, the rotor behaves as a rigid body and is relatively easy to accelerate to speed; however, it has a tendency at full speed to exhibit gyroscopic precessions. Finally, if the length-diameter ratio is very large, the rotor becomes easy to stabilize gyroscopically, but it is difficult to get it to speed because long rotors are very flexible and have resonant frequencies of flexure lower than the operating speed. The problems of these three types of centrifuge (the rotor dynamics, the bearings used to support the rotor, and the stress analysis of the rotating components) were investigated in the last century as part of classical mechanics because of the emergence of steam turbines during the latter part of the industrial revolution. These early principles are briefly reviewed, with particular reference to the work of De Laval, who invented the principle of self-balancing, Reynolds and Evershed, who developed hydrodynamic and magnetic bearing, respectively, and Chree, who did the most extensive early work on the stress analysis of tubes and discs. The work is described as it applies to the centrifuges developed in America and Germany during the war and in the Soviet Union after the war. The work of Beams in America is described in most detail, since he and his colleagues developed all three types of centrifuge during the Manhattan Project. The other work described is that of Groth and Beyerle, who developed subcritical machines in Germany during the war, and of Steenbeck and Zippe, who helped to develop both subcritical and supercritical centrifuges in the Soviet Union after the war. Little of this latter work has been published, but Zippe redeveloped the subcritical machine at the University of Virginia. The description of this machine concludes the present review.

CONTENTS

List of Symbols	67	Acknowledgments	85
I. Introduction	68	Appendix A: The Rosette Rotor	85
II. The Centrifuge Rotor	69	Appendix B: The Jeffcott Analysis of Self-balancing	85
III. Rotor Dynamics of Subcritical Machines and Principle of Self-balancing	70	1. Symmetrical rotor	85
A. Effect of unbalance	70	2. Asymmetrical rotor	87
B. Historical work of De Laval	70	Appendix C: Methods of Damping	87
C. Natural resonances	71	Appendix D: Conical Mode of Precession for Subcritical Rotors	88
D. Synchronous whirls and critical speeds	72	Appendix E: Methods of Achieving Convection-Free Operation	89
E. Jeffcott theory	72	1. Hydrogen stabilization	89
F. The stiffness and damping parameters	73	2. Vacuum operation	90
IV. American (Manhattan) Project	73	Appendix F: Bearing Systems	91
A. Length-diameter ratio	73	1. Hydrodynamic bearings	91
B. Short bowl rotors	74	2. The Evershed bearings	92
C. Subcritical rotors	75	a. Pivot bearing	92
D. The first subcritical centrifuge	75	b. Magnetic bearing	93
E. Westinghouse subcritical centrifuge	76	Appendix G: Stress Analysis of Discs	95
V. Supercritical Rotors	77	References	95
A. Definition of critical speeds	77		
B. Calculation of flexural critical speeds	78		
C. Damping forces	79		
D. Manhattan supercritical centrifuge	79		
VI. The German Project	80		
A. Early machines	80		
B. Postwar machines	81		
VII. Principles of Bearings	82		
VIII. Russian Machines	82		
A. Bearing system	83		
B. Rotor dynamics	83		
C. The hex system	83		
IX. Postscript	84		
A. Stress analysis	84		
B. High-strength materials	84		

LIST OF SYMBOLS

<i>A</i>	area
<i>A</i>	amplitude at cylindrical critical
<i>B</i>	amplitude at conical critical
<i>C</i>	amplitude at top of asymmetrical rotor
<i>C_v</i>	specific heat per mole
<i>D</i>	amplitude at bottom of asymmetrical rotor
<i>D</i>	diameter of bearing
<i>E</i>	Young's modulus
<i>F</i>	magnetic force
<i>I</i>	transverse inertia about <i>C</i> of <i>G</i>

I_1	transverse inertia, $\frac{1}{3}$ down rotor	ϵ_r	radial strain
I_2	transverse inertia about bottom end	η	viscosity
K	stiffness between masses in dynamic absorber	θ	coordinate
L	length between bearings	κ	thermal conductivity
\mathcal{L}	bearing length	λ	thickness ratio of De Laval disc
\hat{L}	length of molecular pump	μ	damping constant in symmetrical system
M	large mass in dynamic absorber	μ_1	damping constant at bottom of asymmetrical rotor
\mathcal{M}	shaft mass	μ_2	damping constant at top of asymmetrical rotor
\hat{M}	molecular weight	ν	Poisson ratio
P	polar inertia of rotor	ρ	density
\mathcal{P}	power	σ	stress
Q	specific load	σ_e	equivalent uniaxial stress
Q_1	mean specific load	σ_r	radial stress
R	gas constant	σ_h	hoop or circumferential stress
R_F	ratio of forces	ω	angular speed
S	bearing stiffness	ω_0	maximum operating angular speed
S_1	stiffness at bottom of asymmetric rotor	ω_1	natural cylindrical frequency
S_2	stiffness at top of asymmetric rotor	ω_2	low-speed approximation of ω_4
T	temperature	ω_3	high-speed approximation of ω_4
U	bearing velocity	ω_4	natural conical frequency
δU	separative work	Δ	center-of-mass shift
V	peripheral velocity of rotor	Δ_1	center-of-mass shift in couple unbalance
V_d	peripheral velocity of De Laval disc	Ψ	elastic constant
V_n	peripheral velocity at n th flexural critical	Ω_1	cylindrical critical in symmetrical system
W	bearing load	Ω_2	conical critical in symmetrical system
$X\omega^2$	force unbalance	Ω_3	low conical critical in asymmetrical system
$Y\omega^2$	couple unbalance	Ω_4	high conical critical in asymmetrical system
Z	rotor length		
b	outer radius of contact in pivot bearing		
d	rotor diameter		
e	eccentricity of manufacture		
f	friction coefficient		
g	mass ratio in dynamic absorbers		
h	gap		
k	stiffness		
l	half bearing separation		
m	mass		
(m_1r)	unbalance		
n	number, 1,2,3, etc., of critical		
p	pressure		
p_1	low pressure in molecular pump		
p_2	high pressure in molecular pump		
q	permeance		
r	radius of rotor		
r_1	radius of cup in pivot bearing		
r_2	radius of pin in pivot bearing		
t	thickness		
v	velocity ωy in damper		
y	radial movement in damper		
z	$y + ix$		
$(\alpha\beta)$	separation factor		
β	molecular velocity		
γ	C_p/C_v		
δ	phase angle		
ϵ	separation efficiency		
ϵ	strain		
ϵ_a	axial strain		

I. INTRODUCTION

All of the high-speed centrifuges reviewed in this paper use the principles first enunciated by Gustave de Laval in 1889. De Laval, one of the great engineers of the last century, became famous as "the man of high speed" and spent most of his scientific life developing high-speed machinery. First, he developed the method of separating cream from milk using a centrifuge which was fifteen times faster than any previous machine. The project, started in 1877, was an almost instant success, and within three years he had founded his now world-famous company which revolutionized the dairy industry. He followed this up by his development of the high-speed reaction turbine, making several important inventions. The important contributions in the present context were the optimum shape of disc for high-speed application, and, even more significant, his principle of self-balancing.

At about the same time that De Laval was developing his ideas on high speed, work was proceeding on the theory and practice of bearings, including magnetic and pivot bearings, and also on the stress analysis of rotating bodies. The milestones of the work, as relevant to the three centrifuge projects reviewed, are given in Table I. The three subjects listed in the table, rotor dynamics, bearing technology, and stress analysis are now specialized disciplines, but in the nineteenth century they formed a natural part of classical science; even now the basic

TABLE I. Milestones in development of high-speed rotation.

Bearings	
1883	Discovery of hydrodynamic lubrication (B. Towers)
1886	Theory of lubrication (O. Reynolds)
1891	Development of pivot and magnetic bearings (S. Evershed)
1904	Theory of journal bearing (A. Sommerfeld)
Rotor dynamics	
1877	The first centrifuge (G. De Laval)
1877	Flexural vibration of rotor (summary) (Lord Rayleigh)
1883	Invention of tuned dampers (P. Watts)
1889	The principle of self-balancing (G. De Laval)
1919	Theory of self-balancing (A. H. Jeffcott)
1928	Optimization procedure for tuned dampers (J. Ormondroyd and J. Den Hartog)
Stress analysis	
1850	Theory of rotating discs (J. Clerk Maxwell)
1891	Complete theory of rotating discs (C. Chree)
1896	Development of optimum disc (G. De Laval and J. Smith)

scientific principles of these disciplines remain unchanged. For example, there is very little difference in design philosophy between the De Laval centrifuge used to separate cream from milk in 1879 and the first centrifuge used by Beams in 1936 to separate the chlorine isotopes, to be followed later by centrifuges for the separation of the uranium isotopes. These early machines of De Laval and Beams were sufficiently short to be gyroscopically stable with bearings at only one end of the rotor. However, short rotors have a limited output, and Beams soon developed machines with rotors of length several times their diameter. These longer rotors needed special damping devices to prevent gyroscopic precession, but were sufficiently short to spin as rigid bodies and operate below their first flexural critical speed.

The work started by Beams at the University of Virginia in 1934 was soon integrated into a much larger program as part of the wartime Manhattan Project in late 1940. The work done during this project is by far the most extensive in the published history of the gas centrifuge; in just four years the scientists at Virginia, with colleagues at Westinghouse and Standard Oil, developed various types of centrifuge, including a much larger version of the Beam's subcritical machine and an even larger supercritical machine about three meters long. These machines were all operated in UF_6 , and the separation results confirmed the general correctness of the Cohen theory of separation, also developed during the Manhattan Project.

At the same time as the Manhattan Project in America there was a smaller but similar program of work underway in Germany. The subcritical machines developed during this project are also described in this review. These wartime machines developed in America and Germany were very similar, mainly because of a similar philosophy of design regarding the bearings and the hex feed

system. However, the postwar machines developed in the Soviet Union and later by Zippe at the University of Virginia used a different bearing and hex feed system, and the machines, although much smaller, were also much simpler. The principles of these various machines are described in this review, but for obvious national and commercial reasons there is no discussion of the major investigations of the gas centrifuge presently underway in the UK, Germany, and Holland (under the auspices of Urenco) or of the work in America or Japan.

II. THE CENTRIFUGE ROTOR

Before discussing the mechanical principles of the centrifuge, it is important to consider briefly the first and most difficult problem—the specifications of the rotor. In particular, there is no clear indication from centrifuge theory as to the best values for the rotor radius, thickness, or length. Indeed it is not even certain that a simple cylinder is the best shape for a centrifuge rotor. This latter point is discussed in Appendix A. The difficulty of choosing the best dimensions for even a simple cylindrical shape follows from the relationships between the separation equations and the mechanical expressions relating to peripheral speed and rotor length. These relationships are such that the important rotor dimensions of length, diameter, and thickness all cancel out.

Consider first the two most important equations in centrifuge technology, which relate to the peripheral speed. First, in the separation theory, there is the Dirac equation,

$$\delta U \sim \epsilon Z V^4, \quad (1)$$

which shows that the output of a centrifuge increases only with rotor length and peripheral speed. The equivalent

theory in stress analysis, which defines the allowable peripheral speed of a rotor, dates back well into the history of elasticity. This theory was summarized by Chree (1891), who gave the most quoted equation in high-speed technology:

$$V^2 = \sigma / \rho . \quad (2)$$

This equation, which will be discussed later, shows that the maximum peripheral speed of rotation of a thin-walled cylinder depends only on the ratio of the acceptable working strength to density of the material of which the rotor is constructed. It is independent of the diameter and thickness of the rotor.

Second, the separation and mechanical equations regarding the rotor length give expressions only for the length-diameter ratio of the rotor. Thus the Cohen equation for the separation factor of a countercurrent centrifuge is of the form

$$(\alpha\beta) = f(\sqrt{\epsilon} V^2 Z / d) , \quad (3)$$

and the equation in rotor dynamics which relates to length—say, for a subcritical rotor—can be written as

$$Z / d = \frac{1.85}{V^{1/2}} (E / \rho)^{1/4} \quad (4)$$

which equals 7 at 350 m/sec for an aluminum alloy rotor. This equation, as well as a similar equation for supercritical rotors which differs only in the constant, gives no direct information on the rotor length, diameter, or thickness.

The only direct information that can be derived from the mechanical equations (2) and (4) is that the material of the rotor should be of high specific strength for maximum peripheral speed and also be of high specific (flexural) modulus for maximum length-diameter ratio. Then, for a given plant output, the separation equation (1) gives a good estimate of the total length of all the rotors added together, and the separation equation (3) shows that it is desirable for each rotor to be of a high length-diameter ratio.

This lack of information on the rotor diameter and thickness is attested to by the widely differing values for rotor diameter and thickness chosen by Beams, Groth, and Zippe and given in Table II. In fact, the values chosen for the radius and thickness of the rotor are more closely related to the more mundane properties of the bearings and dampers used to support the rotor, as will become clear in the following narrative.

TABLE II. Approximate rotor dimensions of practical machines. ($V=350$ m/sec, maximum output 4 kg SW/yr m.)

	Beams/Groth	Zippe
Diameter (mm)	200	76
Thickness (mm)	12.7	1.27
Mass (kg/m)	20	1

III. ROTOR DYNAMICS OF SUBCRITICAL MACHINES AND PRINCIPLE OF SELF-BALANCING

A. Effect of unbalance

The main difficulty in spinning rotors at high speed is the engineering impossibility of making a perfectly balanced rotor, one in which the geometric and mass axes coincide. The net unbalance is usually measured either in units of $m_1 r$, the balance mass required at a given radius of application, or $\mathcal{M}\Delta$, the rotor mass \mathcal{M} multiplied by the distance Δ of the center of gravity from the geometric center. The two are of course equal. Unbalance creates a rotating radial load of $m_1 r \omega^2$ or $\mathcal{M}\Delta \omega^2$, which can easily destroy the bearings or wreck the shaft. This problem is particularly troublesome in the case of a hollow body like a centrifuge because it can have its center of gravity considerably displaced from its geometric center if the central hole is at all eccentric. A simple calculation of the center of gravity gives this displacement as

$$\Delta = er / 2t , \quad (5)$$

showing that the error manufacture—the eccentricity between the inner and outer radii—is magnified by the ratio of radius to wall thickness.

In principle the resulting rotating load can be decreased by careful balancing, but inspection of numerical values shows that this is not easy for very-high-speed application. For example, at 1000 rev/sec the rotating unbalance force is ten times the rotor weight for a Δ value of only $25 \mu\text{m}$ (1×10^{-3} in.). This load could readily be decreased by a factor of 10 or so by precision balancing, but, as will become clear, it can be decreased by several orders of magnitude by the De Laval method of self-balancing.

B. Historical work of De Laval

The principle of self-balancing requires the provision of suitable flexibility in the rotor-bearing system, so that the rotor can find its own center and run about its center of gravity. This principle was established by De Laval (1889), who was becoming exasperated by frequent failures of the bearings and shafts of his steam turbine. According to his biographer, Jung (1957), De Laval discovered the way to achieve self-balancing on 17 February 1889, when, almost as a last resort, he replaced the usual steel shaft of this turbine disc with a flexible rattan cane. The experiment was successful in that the turbine wheel centered itself and ran without vibration when the speed was increased beyond the resonant or critical speed caused by the use of the flexible shaft. Following this experiment, De Laval developed the system as a standard feature in his steam turbine, mounting the turbine wheel on flexible steel shafts; the stiffness was usually adjusted to give a frequency of vibration about a sixth or seventh of design speed, and the shafts were mounted in self-aligning, but otherwise conventional, journal bearings. This arrangement is shown schematically in Fig. 1(a).

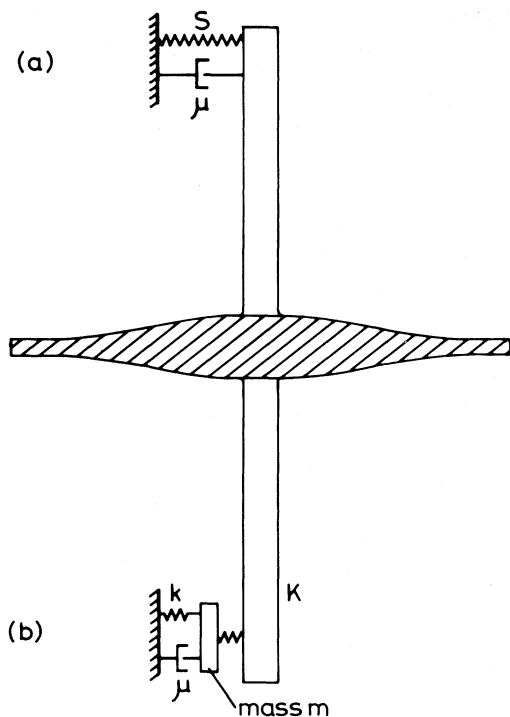


FIG. 1. De Laval turbine disc on flexible support: (a) direct support to earth, using the flexible shaft in series with a flexible damped lubricant film in a journal bearing; (b) indirect damping, using flexibly mounted bearings.

The system developed for his centrifuge was rather different. Here most of the flexibility and damping was in the mounting of the bearings, as indicated in Fig. 1(b). This system is very similar to the dynamic vibration absorber and will be discussed later in the paper.

Surprisingly the mathematical theory of the self-balancing mechanism was not worked out until 1919 by Jeffcott, but it must have been understood in its main essentials almost from its inception. It is clear from the work of De Laval that, for the technique to work, the rotor system must be deliberately designed to have natural frequencies of resonance considerably below the operating speed, and these resonances must be traversed on run-up from rest to full speed. It is the phenomenon which occurs as the rotational speed approaches and then passes the natural resonances which is the basis of the Jeffcott analysis of self-balancing. However, before discussing this balancing effect, it is necessary to define the modes and frequencies of these natural resonances, and to introduce the concept of critical speeds.

C. Natural resonances

Consider first a symmetrical system. The possible modes of whirling of the rotor are shown in Fig. 2(a). The vibrations in which the spinning rotor remains parallel to the axis are called cylindrical whirls and those in which it tilts about its center of gravity are called conical whirls. In both cases the whirls can be in the direction of

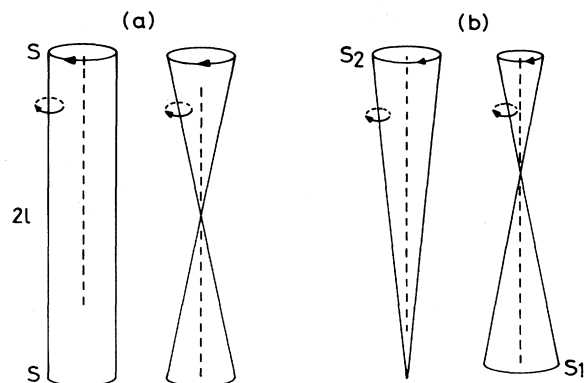


FIG. 2. Cylindrical and conical modes of whirl: (a) symmetrical bearing and rotor; (b) asymmetrical bearing and rotor.

rotation (forward whirl) or opposed to the direction of rotation (backward whirl). This is easy to understand when the rotor is at rest; then the whirls can be considered as two vibrations at right angles, which can combine in either a forward or a backward direction. The frequency is given by the standard solution for simple harmonic motion,

$$\omega_1 = \pm(2S/\mathcal{M})^{1/2} . \tag{6}$$

The positive and negative signs denote the forward and backward whirls. These natural cylindrical whirls can be excited at rest or at any frequency of rotation of the shaft, but will always occur at the frequency given by Eq. (6).

The frequencies of the conical whirls are also very easy to calculate if the rotor is at rest. Taking moments about the center of gravity gives the equation

$$I\ddot{\theta} = -2Sl^2\theta ,$$

where the term on the right-hand side is the restoring couple from the bearings. The solution gives

$$I\omega^2 = 2Sl^2 . \tag{7}$$

Thus the conical frequencies at rest or at very low speeds are given by the equation

$$\omega_2 = \pm(2Sl^2/I)^{1/2} , \tag{8}$$

where the positive and negative signs again denote the forward and backward whirls, respectively.

However, unlike the cylindrical eigenmodes, the frequency of these conical vibrations changes with rotational speed because of gyroscopic effects. Gyroscopic effects will only be touched upon in this review, but they are of considerable importance in the design of high-speed machinery. The main problem is that although the mathematics of gyroscopic motion is reasonably straightforward, it is extremely difficult to follow the underlying physics. The authors of a recent review of gyroscopic effects, Arnold and Maunder (1961), remark rather ruefully that although most of the mathematical theory was developed in the 18th century, mainly by Euler, it is still extremely difficult to explain the physical principles. Be-

cause of this, most of the important gyroscopic properties of the centrifuge will be ignored in this review. However, the effects cannot be neglected for the conical modes of vibration, but at least in this case the basic theorem of gyroscopic phenomena can be used to give a simple explanation. This theorem is that a couple of $P\omega_3$ is required to make a rotor of angular momentum $P\omega$ precess at angular velocity ω_3 , and that all three vectors are at right angles. At high speeds this gyroscopic torque can be so great that the bearing restoring couple can be neglected, and the simple harmonic solution (7) becomes

$$I\omega_3^2 = P\omega\omega_3. \quad (9)$$

Thus the high-speed approximation for the frequency of the forward conical natural modes is given by

$$\omega_3 = P\omega/I. \quad (10)$$

The trivial solution $\omega_3 = 0$ is the asymptotic value, at high speeds, of the backward conical mode. The general solution allowing for both bearing and gyroscopic torques is obtained by solving the quadratic equation

$$I\omega_4^2 = P\omega\omega_4 + 2Sl^2 \quad (11)$$

or

$$\omega_4^2 = \omega_3\omega_4 + \omega_2^2,$$

giving

$$2\omega_4 = \omega_3 \pm (\omega_3^2 + 4\omega_2^2)^{1/2}. \quad (12)$$

This solution, derived by more rigorous methods in standard texts such as the review of Arnold and Maunder (1961), is plotted in Fig. 3. The solution gives the frequencies of the two conical natural modes of vibration as a function of rotational frequency, and as can be seen, the gyroscopic effects dominate in the case of the forward

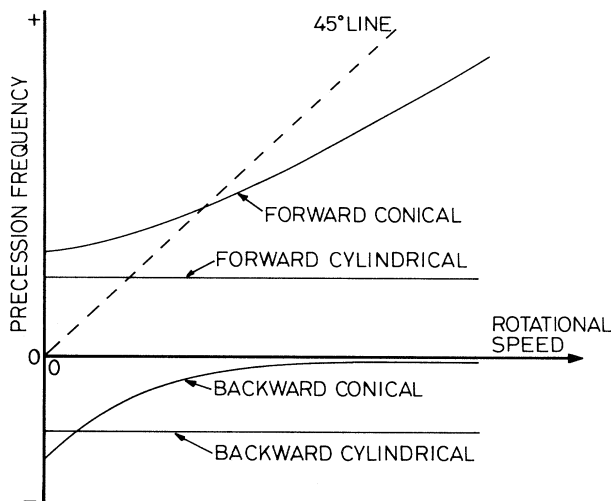


FIG. 3. Variation of conical and cylindrical whirl frequencies with rotational frequency. These curves are for a symmetrical system. The changes in frequency for the conical mode are due to gyroscopic effects. The points of intersection with the 45° line give the frequencies of the rigid-body criticals.

conical whirl. For completeness the frequencies of the cylindrical modes, Eq. (6), are also plotted in this figure. These four natural modes of vibration can be excited at any frequency of rotation, but will always occur at the frequencies given by Eqs. (6) and (12) and not at the frequency of rotation. On this account they are sometimes called asynchronous whirls to distinguish them from the synchronous whirls excited by the unbalance forces involved in the discussion of critical speeds.

D. Synchronous whirls and critical speeds

Using Fig. 3 it is easy to calculate the critical frequencies at which the rotational frequency equals the frequencies of the natural modes of vibration. Thus as the speed of the rotor is increased, its rotational frequency follows the 45° line, and the points of intersection with the positive solutions of Eqs. (6) and (12) give the critical conditions. At these frequencies, sometimes called critical speeds, the amplitude of rotor whirl can attain dangerous proportions. The exact frequencies of the criticals can be obtained by solving for the intersection points, giving the frequencies of the cylindrical and conical critical speeds as

$$\Omega_1 = (2S/\mathcal{M})^{1/2}, \quad (13)$$

$$\Omega_2 = [(2Sl^2)/(I-P)]^{1/2}. \quad (14)$$

Most rotors have to traverse these two rigid-body criticals as they are run up to full speed. The first critical is excited by the unbalance force acting at the center of gravity and the second by any couple unbalance about the center of gravity. The conical critical clearly does not exist if the polar inertia P is greater than the transverse inertia I , and if it does exist it is not traversed if the operating speed is less than that given by Eq. (14).

E. Jeffcott theory

The effects of traversing these critical speeds were first analyzed by Jeffcott in 1919, and a full discussion of his approach is given in Appendix B. However, the physical principles can be seen by considering the balance of forces as a symmetrical rotor is increased in speed and traverses the cylindrical critical speed. The sequence of events is as follows.

(a) At low speeds the radial displacement is nearly in line with the unbalance force $\mathcal{M}\Delta\omega^2$, and the amplitude of whirling is given by the balance between the centrifugal force and the bearing restoring force $2S\mathcal{A}$,

$$\mathcal{A} = \mathcal{M}\Delta\omega^2/2S. \quad (15)$$

(b) As the speed is increased the displacement lags behind the unbalance force (because of the effect of damping); eventually the phase angle is 90° at the critical frequency, and the displacement, of nearly maximum magnitude, is at a right angle to the unbalance vector. At this critical speed, when the phase angle is 90°, the bal-

ance of centrifugal force and the damping force, $2\mu\mathcal{A}\Omega_1$, gives the deflection

$$\mathcal{A} = \mathcal{M}\Delta\Omega_1/2\mu. \quad (16)$$

This equation is sometimes called the energy equation—see Den Hartog (1934)—because at this condition the energy input from the unbalance equals the energy absorbed by the damper.

(c) Thereafter, as the speed is increased beyond the critical condition, the displacement tends to be opposite to the force, until at high speeds it is 180° out of phase and the rotor runs smoothly about its center of gravity. At this condition the inertial force and centrifugal force balance, giving

$$\mathcal{A} = -\Delta. \quad (17)$$

Thus at full speed the radial deflection of the rotor from its original position, sometimes called the run-out, is the center-of-mass shift Δ . This gives the important result that the radial bearing force at full speed is only the restoring force $2S\Delta$ instead of the full unbalance force $\mathcal{M}\Delta\omega_0^2$. This ratio can be written more simply in terms of the critical speed when a flexible shaft/bearing system is used. Thus, using Eq. (13), the ratio of the forces is given by

$$R_F = 2S\Delta/\mathcal{M}\Delta\omega_0^2 = \Omega_1^2/\omega_0^2. \quad (18)$$

This equation is useful in quantifying the self-balancing principle. For example, in the case of the De Laval design, the critical speed was about one-seventh of the running speed, so the side load was reduced by about 50. In the case of the centrifuge design of Steenbeck and Zippe, the critical speed was only about one-hundredth of running speed, so the radial load was reduced to such a small value—by a factor of 10^4 —that it was possible to use small instrument-type bearings to center the rotor.

This self-balancing principle, which makes possible a large reduction in bearing load, is probably the single most important principle in the design of high-speed machines.

F. The stiffness and damping parameters

The main disadvantage of self-balancing is the result of the very method of achieving it—at least one rigid-body critical has to be traversed. Equation (16) for the amplitude at the critical can be rewritten

$$\mathcal{A}/\Delta = (2S\mathcal{M})^{1/2}/2\mu. \quad (19)$$

This shows that, for a given unbalance, the only parameters which affect the rotor amplitude and can be varied are the stiffness constant and the damping constant. It is essential to adjust these two parameters so that the amplitude at the critical speed is reasonable and does not itself wreck the shaft or bearings.

Normally the stiffness is chosen first; this defines the robustness of the machine and generally helps to minimize changes in the displacement of the rotor relative to

its bearing housings. Clearly in the De Laval turbine and most machine tools using the self-balancing principle—for example, the high-speed gas bearing dentist's drill—it is essential that the rotor not be displaced too much from its normal position by sideways forces. The shaft-bearing system must therefore be reasonably stiff. However, in the case of the centrifuge the rotor can be allowed to deflect by a small amount from its central position, and there is more freedom in the choice of the stiffness used for self-balancing. For example, Beams set his stiffness rather low to give a frequency of the cylindrical whirl at about 5% of running speed, and Zippe set the stiffness so low that the cylindrical whirl was only 1% of running speed. These lower values of stiffness, and hence natural frequency, make the initial design problem much easier because the bearing side load is so much less—see Eq. (18)—but the machine is more fragile and more susceptible to disturbances.

Once the stiffness is fixed, the problem resolves itself into introducing the correct amount of damping into the system. There are three methods of achieving this. The first method, pioneered by De Laval in his steam turbine, is to use the damping inherent in the lubricant film of fixed bearings, and this method is still by far the most widely used in modern machinery. The second method is to use flexibly mounted bearings and provide the damping forces on the outside of the bearing housing. This method was also used, possibly unwittingly, by De Laval in his cream separator, and later by Zippe in his centrifuge. The third method, developed by Beams and Groth, is to use two sets of bearings, one set fixed to earth, to provide the stiffness, and one set floating, to activate an external damper. This method is rather wasteful in energy, but the separation of the two parameters makes it easy to optimize. More details of these three methods are given in Appendix C.

IV. AMERICAN (MANHATTAN) PROJECT

A. Length-diameter ratio

The methods used to provide the stiffness and damping for self-balancing in the American, Russian, and German machines are of great importance and have had an important influence on the relative success of the various designs. In particular, the choice of the stiffness of the shaft-bearing system and the consequent reduction in bearing load have a major effect on the power consumption and on the relative stability of the machines. This will be discussed again later. However, the most obvious visual feature of a machine is not the bearing and damper system, but the length-to-diameter ratio of the rotor, and it is this feature which is used to classify machine types. There are, in fact, three types, and all three were investigated during the Manhattan Project. These are indicated in Fig. 4 and are, in order of simplicity of spinning, the short bowl rotor, the subcritical rotor, and the supercritical rotor. They are easily recognized by inspection; a

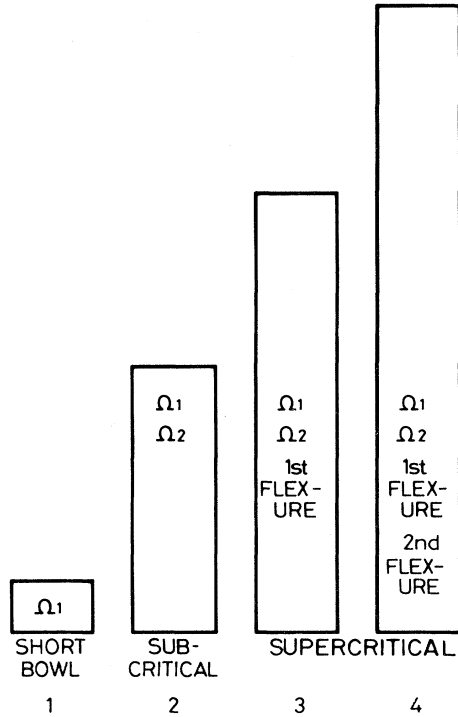


FIG. 4. Rotors of varying length-diameter ratio, from the short bowl rotor, typical of early designs such as that of De Laval, to supercritical rotors, such as those developed during the Manhattan Project.

length-diameter ratio of less than 1 characterizes the short bowl rotor, about 4 or 5 to 1 the subcritical design, and greater than 10 to 1 the supercritical design. Intermediate lengths are not generally used because if a critical is traversed it is only sensible to maximize the length of the rotor without hitting the next critical. Moreover, machines of intermediate length are difficult to spin because the last critical to be traversed is unnecessarily close to operating speed.

B. Short bowl rotors

It was shown earlier—see Eq. (14)—that there is no conical critical speed to traverse on run-up to full speed if the polar moment of inertia of the rotor is greater than its transverse inertia. These favorable gyroscopic conditions apply especially to a disc or a very short tube, both of which have a polar inertia twice the transverse inertia. It is well known that such very short rotors are easy to spin at high speed, and they are sometimes referred to as disc rotors. However, the polar inertia is still greater than the transverse inertia up to a length-diameter ratio of 0.84 or 1.22, depending on whether the tube has end caps¹ or not. Thus rotors shorter than these values have no conical crit-

¹For this calculation the end caps are assumed to be of the same thickness as the tube.

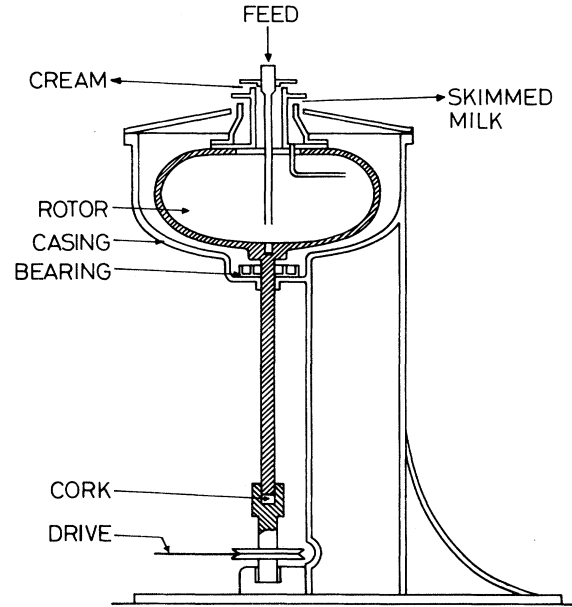


FIG. 5. Short bowl centrifuge, De Laval (1879). The first high-speed centrifuge of De Laval, producing centrifugal force 5700 times gravity, and used to separate cream from milk. Figure is courtesy of the National Science Museum, London.

ical speeds and are reasonably easy to design for high-speed rotation. The centrifuge described by De Laval in 1879 and that of Beams (1936) both fall into this category of design. A schematic of these two machines is given in Figs. 5 and 6, and their dimensions are given in Table II. If anything, the De Laval rotor is the more advanced design, having a useful length-diameter ratio of about 0.45, whereas the Beams centrifuge has a useful length-diameter ratio of only 0.07. The two main differences are

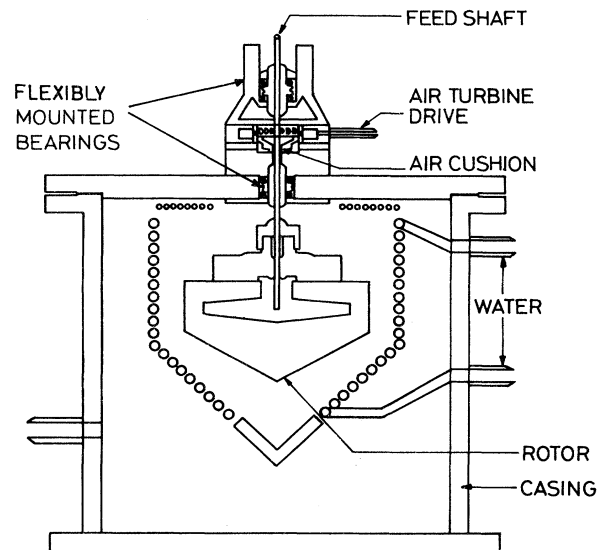


FIG. 6. Short bowl centrifuge, Beams (1936). This centrifuge used to separate chlorine isotopes (1936) and uranium isotopes (1940).

TABLE III. Dimensions of the American centrifuge rotors (including the De Laval rotor for comparison).

Type	Length (mm)	Diam. (mm)	Angular freq. (Hz)	Peripheral speed (m/sec)	Z/d	Thickness (mm)	Material
Short bowl							
De Laval	114	254	117	93	0.45		
Virginia	6.4	89	1550	433	0.07		
Subcritical							
Virginia	280	76.2	1060	253	3.67	12.7	Chrome moly steel
Virginia	356	76.2			4.67		
Virginia	841	166	450	234	5.07		Aluminum ST14
Westinghouse	1067	182.9	470	270	5.83	12.7	Aluminum ST14
Supercritical							
Virginia	857	69.8	885	195	12.28	3.2	Aluminum ST14
Virginia	3450	186.7	350	200	18.5	12.7	Aluminum ST14
Westinghouse	3353	182.9	470	270	18.33	12.7	Aluminum ST14

that, first, the rotor in the Beams centrifuge had a much higher peripheral speed and, second, to minimize convection currents, it operated in a low pressure of hydrogen, requiring fairly complex sealing arrangements.

The first attempts to separate the uranium isotopes were in fact made using this centrifuge in 1940, when about 6 g of UF_6 were centrifuged in the machine, operating in the evaporative mode. However, the samples collected were apparently lost and not measured for isotope abundance. The first experiments including measurements of separation were made about one year later, when more UF_6 was available. The full details of these early measurements, in which a change of isotopic abundance of about 4% was achieved, have been reported extensively by Beams (1975).

C. Subcritical rotors

It was apparent to the Virginian scientists from the beginning that increased length was essential for an increase in the output of the centrifuge. The separation experiments of Beams with the short bowl rotor were only tests of principle. However, as described above, if the length-diameter ratio of the rotor is increased beyond about unity, the transverse inertia becomes larger than the polar inertia; then the conical critical speed given by Eq. (14) falls below the operating speed and has to be traversed on run-up. Similarly, the frequency of the conical natural mode² of vibration falls in the operating speed range, and there has to be some damping available at operating speed to

prevent excitation of this mode.

Fortunately the ratio of transverse to polar inertia increases rapidly with length—to a first approximation I/P equals $\frac{1}{3}(Z/d)^2$; it involves only a small increase in length-diameter ratio to reduce the conical critical to a low value and a not much greater increase to bring the conical natural frequency to a low value. This is discussed further in Appendix D.

D. The first subcritical centrifuge

The first subcritical gas centrifuge developed by Beams (1938) is of historical importance. The rotor dimensions of this machine are given in Table III and, as can be seen, it was not an ideal design since it had a length-diameter ratio of only 3.67. At this length diameter the ratio of polar to transverse inertia is still fairly high, 0.2, so although the conical critical speed is reasonably low, the conical natural frequency from Eq. (10) or (12) is still rather high at 220 Hz, one-fifth of the running speed. Thus in this first centrifuge there was the difficult problem of developing dampers that would both allow the rotor to start smoothly through the low-speed cylindrical and conical criticals at a few Hz, and also prevent any reexcitation of the conical natural mode of vibration at full operating speed.

Despite this difficulty of designing a damper to cover such a wide frequency range, Beams successfully developed his machine and carried out early experiments on the separation of the chlorine isotopes. Following his experience with this rather difficult design, Beams soon developed longer subcritical rotors of length diameter of up to 5.07; the dimensions of some of these rotors are listed in Table III. These rotors, much easier to spin, were

²Remember the distinction between the critical speeds and the natural modes of vibration.

all used for separation experiments culminating in the main Westinghouse machine developed as a possible production machine for the Manhattan Project.

E. Westinghouse subcritical centrifuge

A schematic of the main subcritical machine developed during the Manhattan Project is shown in Fig. 7, and the main dimensions are listed in Table III. Partly because of the larger diameter and partly because of the considerably improved length-diameter ratio of 5.8, the conical natural frequency at operating speed is only 38 Hz. This frequency is not much greater than the critical frequencies, and it is therefore relatively easy to design a damping system which will both allow the criticals to be traversed on run-up and minimize the risk of excitation of the natural frequencies at full operating speed. For example, the damping required for the critical, from Eq. (16), is only about 1000 Nsec/m, and the damping force $\mu\Omega_1 y$ only about 10 N for an amplitude at the critical of 0.1 mm. This damping, allowing very smooth run-up, would normally also be sufficient to control the rotor at full speed unless

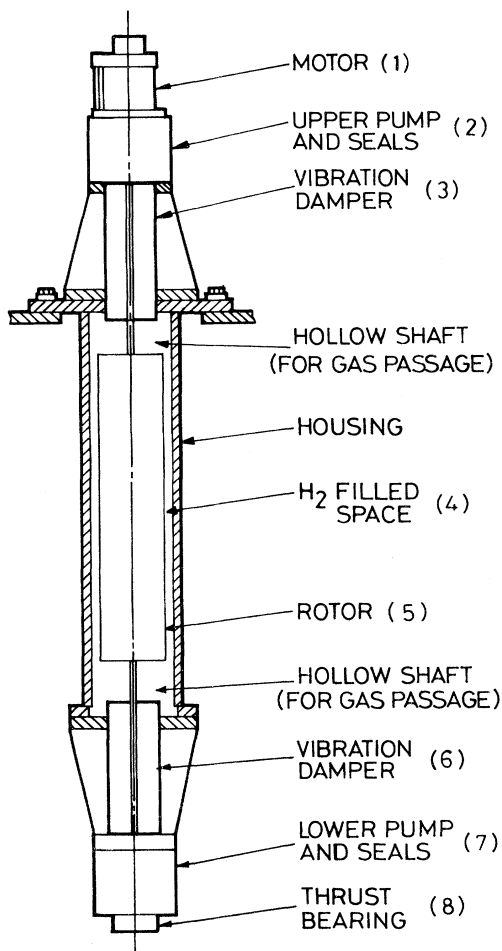


FIG. 7. Westinghouse subcritical centrifuge, developed for production application.

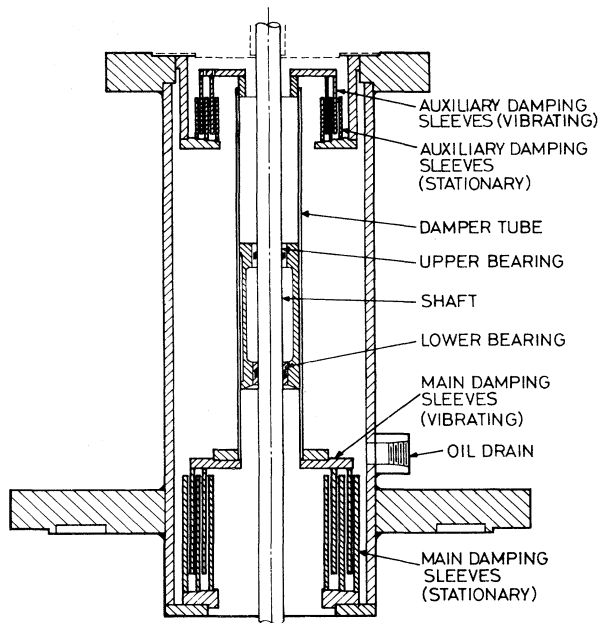


FIG. 8. Upper damper of subcritical centrifuge. Concentric sleeve dampers used in Manhattan Project machines; theory as for a nonrotating journal bearing with a rotating load.

there were very severe disturbing forces.

The damping was provided at the top and bottom of the Manhattan rotor, using a set of concentric cylinders. Concentric sleeves attached to the floating damping bearings were intersticed with concentric sleeves which were attached to the machine frame to form small clearances filled with damping oil. The arrangement is shown in Fig. 8. If the rotating shaft began to whirl it set the cylinders attached to the bearing into a precessional motion, which was resisted by oil flows between the cylindrical surfaces. Each pair of adjacent cylindrical surfaces behaved as a nonrotating journal bearing subjected to a rotating load. Precessional movement was resisted by pressure building up on one side of the bearing with a corresponding drop in pressure on the other side. The average pressure difference multiplied by the projected area of the bearing gave the damping force, the exact calculation being given, for example, by Shaw and Macks (1949).

This part of the Westinghouse design, providing the correct damping, was very successful. There are, however, major disadvantages in this centrifuge design which arise from the method of self-balancing. The flexibility for self-balancing was provided by two fairly long tubular shafts which were connected to, and rotated with, the main centrifuge rotor. The inside of both of these flexible shafts (each consisted of two thin-walled tubes,³ one sup-

³All the Manhattan machines had two entry and two extraction pipes; therefore both the top and bottom flexible support had to be double walled.

ported concentrically within the other) was used to conduct the isotopic gas mixture into and out of the rotor bowl, and the outside was used as the rotating element for the support and damper bearings. This led to an inevitable dichotomy of interests. To give a reasonable gas conduction for the gas flow requires a shaft of large diameter, whereas a low loss of bearing power is more easily achieved using a small-diameter shaft. For example, to transport the hex into and out of the rotor of the Westinghouse machine required a tube of 19 mm outside diameter. The bearings on the outside of the shaft were therefore of large size and consisted of four journal bearings at each end, each of diameter of 19 mm and length 6.3 mm, giving a power loss of 1000 W. The thrust bearing had a loss of 200 W, so that the power loss of the bearings alone was 1200 W.

This power loss itself is quite high, but the main disadvantage of the spinning tubular shaft system is the need for a complex array of rotating seals at each end of the rotor. This array of seals adds to the mechanical complexity of the machine and causes further power loss. In this particular machine there were seals to separate the various oils used for the motor, thrust bearing, journal bearings, and dampers from the hex in the feed and extraction conduits and in the rotor. There were also seals to prevent oil or hex vapor from leaking into the space outside the rotor. Effectively the machine was split into the eight separate spaces shown in Fig. 7.

The most complicated sealing arrangements were in the

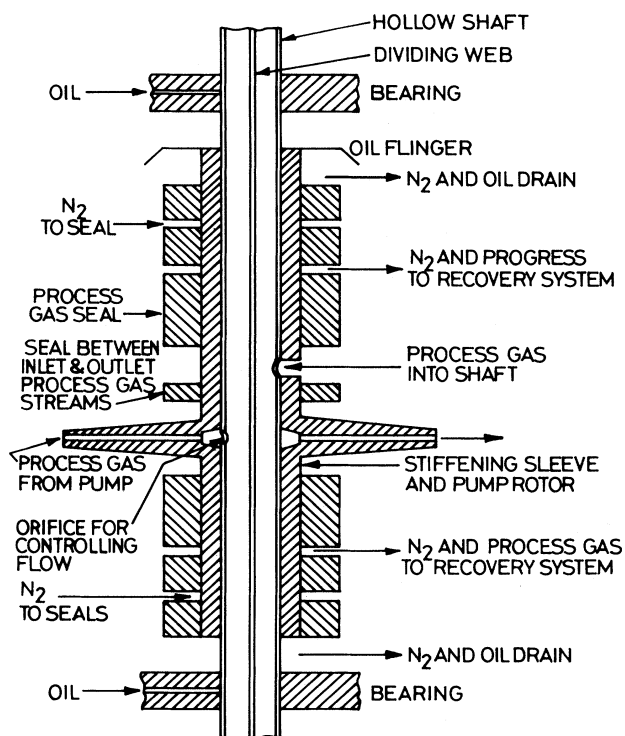


FIG. 9. Schematic arrangement of upper seals and pumps. Complex array of seals caused by using flexible shaft for gas conduits as well as for self-balancing.

spaces (2) and (7), where the hex for feed and extraction were separated from each other and from adjacent oil bearings. This was achieved by using close-fitting rotating seals fed at suitable positions with a buffer gas, dry nitrogen, as indicated in the enlarged schematic in Fig. 9. This diagram is only a schematic; the actual engineering details were rather more daunting, and this is just one of the seal systems.

A second disadvantage of these seals was that they contributed considerably to the power loss. The total electrical usage of the Manhattan machine, including losses in the motor, was about 5 kW. This high power was not only expensive in itself but it tended to set up temperature gradients in the rotating system, giving unwanted convection currents of the process gas in the rotor. To eliminate any such effect the rotor was maintained at a constant temperature by surrounding it with a hydrogen atmosphere at a pressure of about 2000 Pa or 15 Torr. This technique, although it consumed another 100 W or so of power, was extremely effective and is described in detail in Appendix E.

Several of these large subcritical Westinghouse machines were made, and one was operated for 99 days by the Standard Oil Development Company and processed about 500 kg of UF_6 at a maximum and very high separation efficiency of about 85%. The machine eventually developed a leak in January 1944 and was never rebuilt because, at about this time, the project was terminated in favor of the diffusion process.

V. SUPERCRITICAL ROTORS

A. Definition of critical speeds

It is clear from the previous discussion that as the rotor is made longer the problem of the conical vibrations becomes trivial. However, beyond a certain length there is the even more difficult problem of spinning the rotor through one or more flexural critical speeds. The only published designs of supercritical centrifuges are the ones developed during the Manhattan Project, but there are several publications of supercritical operation of conventional machines. In fact, the basic theory of flexural whirling of rotating shafts was studied by many scientists at the turn of the century, and a comprehensive study of this work is given by Gunter (1966) of the University of Virginia.

Two of the most important early papers are by Dunkerley (1894) and Chree (1904), who, although viewing the flexural criticals from different standpoints, came to the same conclusion. The problem, as described by Dunkerley, is that long rotors have resonant frequencies of flexure lower than the operating speed. Therefore, when the rotor is run to full speed there are certain speeds of rotation at which the rotational frequency equals the resonant frequency. At these critical speeds the effect of any unbalance force could be to set the rotor whirling at large amplitudes, causing possible damage or destruction. The

alternative description, similar to that given by Chree, would be from the viewpoint of the experimenter, i.e., a stationary observer. From this viewpoint the restoring force at the criticals, given by the bent shaft, would be unable to provide the centripetal force required for the circular orbit, and the amplitude is only kept under control by damping forces. Whichever definition is used, it is clear that the problem is the same as for the Jeffcott rigid-body criticals described earlier. In fact, the flexural criticals and the rigid-body criticals should be categorized collectively as system criticals, since they merge into one another as a function of the end restraint. The effect is described by Miller (1954), and his results are shown in Fig. 10. However, for the centrifuges described in this review, the bearings have negligible stiffness, relative to the rotor bending or flexural stiffness, and it is permissible to (a) calculate the frequencies of the two "rigid-body" criticals as described earlier, using Eqs. (13) and (14), and (b) calculate the flexural criticals of the rotor assuming the bearings have zero end restraint. The only problem this introduces is that of counting—the first flexural critical is sometimes referred to as the third system critical.

B. Calculation of flexural critical speeds

The first problem, following Dunkerley, is to calculate the natural frequencies of flexure of the rotor. There are

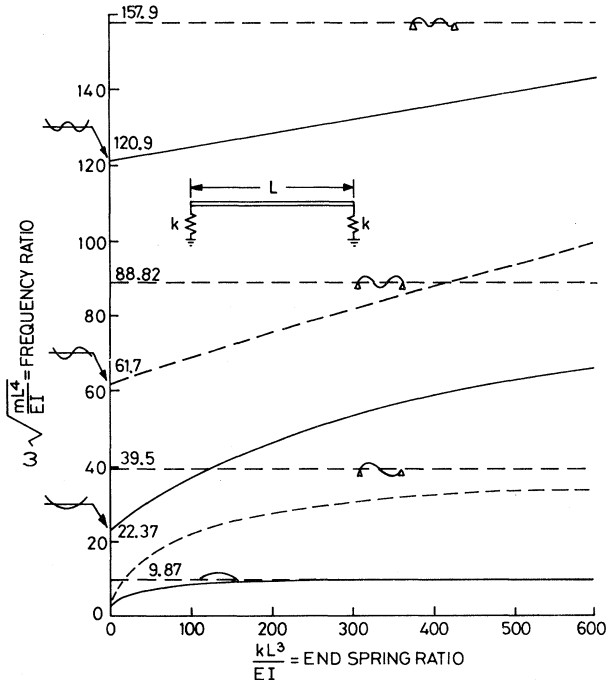


FIG. 10. Natural frequencies of a beam on spring end supports (m =mass/unit length of rotor; I =moment of inertia of area). At low end-spring stiffness the first three criticals comprise two rigid-body criticals and a "free-free" flexural critical. At high-support stiffness all criticals are flexural criticals with minimum movement at rotor ends.

TABLE IV. Length-diameter ratio of aluminum rotors of peripheral speed 350 m/sec (assuming zero cap mass) (from Whitley 1979, courtesy Institute of Physics, London).

Z/d	Critical speeds (m/sec)			
	1st	2nd	3rd	4th
7	400			
11.6	145	400		
16.3	74	204	400	
21	45	123	242	400
25.5	30	83	162	269

both analytical and numerical methods for calculating these frequencies, the most comprehensive modern analysis being that of Bishop and Johnson (1955). The calculations, if done exactly, should also allow for any deflection of the rotor due to shearing forces and for the effects of the gyroscopic couples of the whirling sections. This is described by Timoshenko (1928). However, the physical principles are best understood by ignoring these small effects and using the method developed by Lord Rayleigh (1877) and published in his classic book on sound. This method is to equate the potential energy of the thin tube when at its maximum amplitude with its maximum kinetic energy, which occurs when passing through the unbent condition. The Rayleigh theory, with slight modification, gives the solution for the peripheral velocity at the critical speeds as

$$V_n = \frac{(n + \frac{1}{2})^2 \pi^2}{4(Z/d)^2} \left[\frac{E}{2\rho} \right]^{1/2} \quad (20)$$

This standard Rayleigh equation gives the critical speeds for a given Z/d ratio or, by transposing the equation, the Z/d ratio for a given critical speed. As shown, the critical frequencies and Z/d ratios for thin-walled tubes are independent of thickness but dependent on the specific modulus (E/ρ) of flexure of the material of construction. This specific modulus is much the same for the common high-strength materials such as aluminum, steel, and titanium; in particular, for the aluminum alloys used in the Beams centrifuge it is about $25.5 \times 10^6 \text{ m}^2 \text{ sec}^{-2}$.

Substituting this value in the above equation gives the critical speeds for various length-diameter ratios as summarized in Table IV. As shown, the longest rotor that could operate at 350 m/sec without passing a flexural critical has a length-diameter ratio of seven.⁴ Longer rotors must pass at least one flexural critical speed—for example, a rotor of length-diameter ratio of 16.3, similar to the rotor in the supercritical machine developed during the Manhattan Project, has two flexural criticals at 74 and 204 m/sec and would then operate below the third critical, set by Eq. (20), at 400 m/sec.

⁴Real subcritical rotors are rather shorter than this because of the effect of the mass of the end fittings, ignored in this simplified explanation.

C. Damping forces

The Rayleigh equation gives the frequencies of the flexural critical speeds, but it gives no information regarding the problem of traversing them. Some indication can be deduced from the energy equation (16), which shows that the damping constant required to control the amplitude of a critical speed is proportional to the frequency of the critical, and the damping force is proportional to the frequency squared. Thus the task for supercritical rotors is twice as difficult as that for subcritical rotors, in that not only is the required damping itself much greater, but it has to be provided at a much higher frequency.

The more exact calculations of Miller (1954) show that the optimum damping for the flexural criticals, given as a constant times $M\omega$, is a little less than that given by Eq. (16). This is because the effective mass of the vibrating rotor to be used in the equation reduces for increasing mode number. Thus the optimum damping for the first flexural critical is about $0.2M\omega$, where ω is the angular frequency of rotation of the critical. This damping applied at each end of the rotor restricts the bend of the tube at its first flexural critical to about double the initial value. The optimum damping for the higher criticals is greater because of the higher frequency, but at least the constant is reduced in approximate proportion to the number of the critical, i.e., it is 0.1, 0.066, and 0.05 for the second, third, and fourth criticals, respectively.

D. Manhattan supercritical centrifuge

These principles of supercritical design are exemplified by the two big supercritical machines developed at the University of Virginia and at Westinghouse during the war. The rotors in these two machines were of virtually identical dimensions, 3 m in length and 0.2 m in diameter. The important dimensions are given in Table III, and a schematic of the Westinghouse machine is given in Fig. 11. A comparison of Figs. 7 and 11 shows that the ends of the Westinghouse subcritical and supercritical machines are similar. In particular, the design of the seals is virtually identical, and these need not be described further. The main difference between the two machines is in the value of the damping that is required for successful negotiation of the various critical speeds. The subcritical rotor has only to negotiate the two rigid-body critical speeds at 10 and 30 Hz, whereas the supercritical rotor also has to traverse two flexural critical speeds at 100 and 300 Hz. The actual values of damping constant used in these Westinghouse machines are not quoted in the literature, but the values can be estimated from the simplified principles given in this review and these estimates are given in Table V.

The problem of achieving the high damping forces required for supercritical operation was avoided in the centrifuge at Virginia. The damping was not optimized. Instead a 33 kW steam turbine was connected to the lower

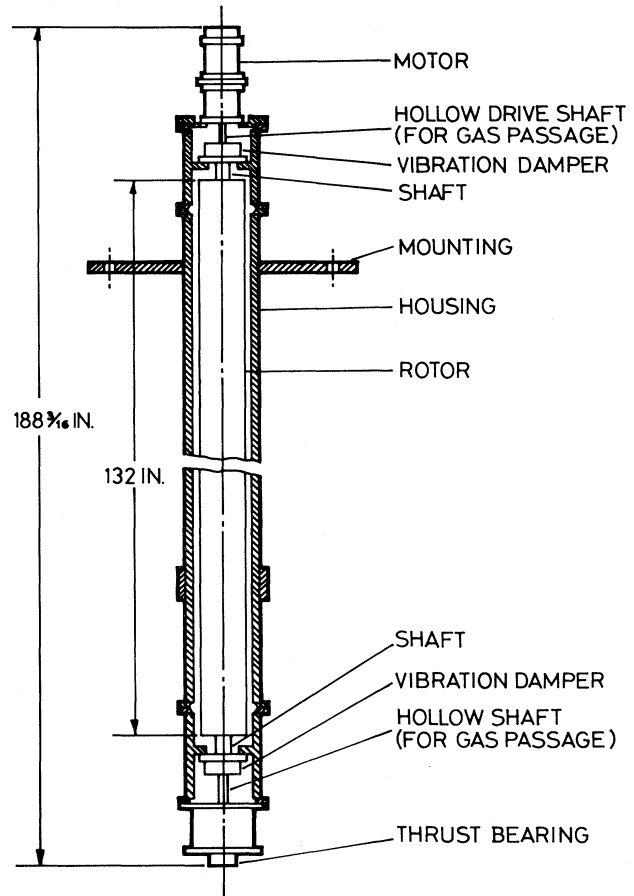


FIG. 11. Manhattan Project supercritical centrifuge.

end of the centrifuge, and it was rapidly accelerated through its two flexural criticals, giving no time for the amplitudes at the criticals to build up to dangerous levels. In this way the machine at Virginia was successfully spun to full speed (350 Hz) and extensive separation measurements made from September 30, 1943 to January 31, 1944.

This method of achieving full speed was acceptable for a laboratory machine in which the main objective was to obtain separation measurements to confirm the separation theory. However, the Westinghouse machine was required as a production machine, with its power limited to about 5 kW, and it was therefore necessary to optimize the dampers. The Westinghouse scientists had no difficulty in designing the dampers to pass through the two rigid-body criticals and the first flexural critical at about 100 Hz. However, optimization for the second flexural critical at 300 Hz was more difficult because the dampers suffered from cavitation problems.

The actual damper used is shown in Fig. 12. As described earlier, these dampers resist precessional movement by building up pressure on one side with a corresponding drop in pressure on the other side. For the heavy damping force required for the second flexural critical, the pressure drop was larger than the available pres-

TABLE V. Comparison of Westinghouse subcritical and supercritical machines [power and force assume in each case a precession amplitude of 0.1 mm, and damping for cylindrical critical from Eq. (15) to give $\mathcal{A}/\Delta = 5$].

	Units	Subcritical	Supercritical
Length	meter	1.07	3.35
Mass	kg	33	85
Cylindrical critical			
Frequency	Hz	16	16
Damping constant	N sec/m	660	1700
Damping force	newtons	6.7	17
Damping power	watts	0.067	0.17
Conical critical			
Frequency	Hz	30	33
Damping constant	N sec/m	310	880
Damping force	newtons	5.9	18
Damping power	watts	0.11	0.38
First flexure critical			
Frequency	Hz		100
Damping constant	N sec/m		10 700
Damping force	newtons		670
Damping power	watts		42
Second flexure critical			
Frequency	Hz		300
Damping constant	N sec/m		16 000
Damping force	newtons		3000
Damping power	watts		570

sure head, and cavitation occurred. It was found during the experiments that this cavitation could be inhibited by increasing the ambient pressure—indeed, it was found that the damping could be increased about tenfold by increasing the pressure in the damper housing from about 3.5 to 55 kPa (0.5–8 psi). Several attempts were then made to accelerate the rotor through the second critical using this housing pressure as a means of damping control. In these trials, if the rotor failed to accelerate through the critical speed, the limited power available prevented any serious damage; the damping power equalled 5 kW at an amplitude of 0.3 mm, thus making the test self-limiting. By careful coaxing, and adjustment of the damping pressure, the test engineers did eventually succeed in passing the second critical and accelerating this large rotor to full test speed. Once past the critical the rotor ran very smoothly.

However, run-down is, or actually was, a different

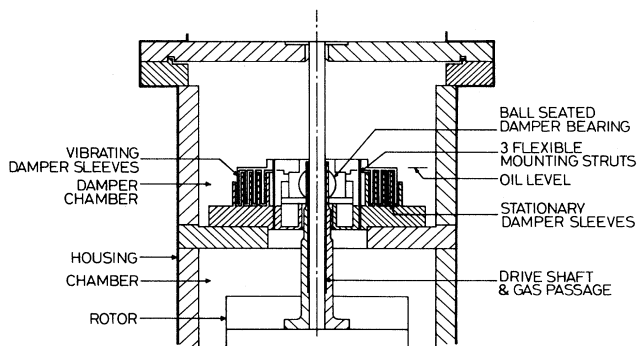


FIG. 12. Upper damper of the supercritical centrifuge.

matter. One has only one chance to get the damping right; if it is incorrect, the amplitude of the vibrations can increase to dangerous levels. On run-down there is no limit from power considerations because of the large amount of kinetic energy available in the rotor, in this case 100 000 J for a 10-Hz reduction in speed at the critical. Unfortunately, on run-down of this first Westinghouse prototype and on approaching the critical, the amplitude of rotor whirl did increase beyond an acceptable limit, causing a crash which completely wrecked the centrifuge. This crash coincided with the cancellation of the centrifuge project, and so the machine was never rebuilt. The timing was unfortunate in that it would have been relatively straightforward to develop the damper to be of the same value on run-up and run-down.

January 1944 was thus an eventful month for the American centrifuge project. Researchers at Virginia were completing their separation measurements on their large supercritical machine, the subcritical machine on life test at Standard Oil had operated continuously for 100 days and then developed a leak, and the Westinghouse supercritical machine crashed; then as a final blow the project was canceled when on the brink of success.

VI. THE GERMAN PROJECT

A. Early machines

At much the same time as the above machines were being developed during the Manhattan Project in America a similar program of work was underway in Germany. The

centrifuges were initially developed by Groth of Bonn University and Beyerle of the gyroscope firm of Anschütz and Co., Kiel. Their first designs, the UZ1 and the UZ111B, followed the same principles as the early designs of Beams (1938), in that the flexible shafts used for the self-balancing mechanism consisted of thin-walled tubes, the inside used for gas passages to the rotor and the outside for support bearings and damper bearings. The tubular shaft connected to the top of the rotor provided the feed passage and one exit passage for the gas, and it was also connected to a drive motor at the top. The tubular shaft at the bottom served as the second gas exit passage, but since the German machines were developed on the single feed system this shaft did not need to be double walled.

The rotors, of dimensions given in Table VI, were thick-walled cylinders made of a high-strength aluminum alloy, Bondur, and most experiments were made at peripheral speeds of 252 and 280 m/sec. As with Beams's machines, there was a complex array of bearings, dampers, and seals at each end and on the outside of the flexible shafts. These seals have been described in several papers, for example by Groth (1961), and need not be described here. Again, as with the Manhattan machines, there was a high power loss, about 2 kW, creating the possibility of unwanted temperature gradients and therefore undesirable countercurrents, which could diminish or destroy the separation effect. The solution to this problem in the German machines, as in the Manhattan machines, was to introduce hydrogen into the casing, so maintaining the rotor at a constant temperature. This work on the temperature stabilization of the wartime German machines has been described in detail by Groth and Beyerle (1958) and is summarized in Appendix E.

B. Postwar machines

The German work on centrifuges continued after the war. The first machine developed, the ZG3, incorporated a number of design improvements, mainly relating to the design of the flexible supporting shafts, the dampers, and the bearing power consumption. The dampers have been described in detail by Groth (1957); in the final machine they limited the maximum amplitude of oscillation of the

rotor to 0.1 mm. The power consumption was reduced to about 1.7 kW at the slightly higher speed of 300 m/sec. As before, hydrogen at a pressure of a few hundred pascals was used in the casing, of gap 4 mm, for temperature stabilization. The ZG3 also included for the first time a technique, with external control, for setting up a temperature difference between the top and bottom end caps, to set up the thermal countercurrent. The top end cap was heated using eddy currents generated by a small electromagnet, and the heat was extracted by a ring-shaped cooler below the bottom cap.

This arrangement was also used in the ZG5, the last machine developed by Groth and his associates. The ZG5 incorporated two other major improvements. First, as shown in Table VI, the machine was much longer, simplifying the problems of rotor dynamics, and second there was a change in design principles regarding the method of gas feed and extraction. In all the previous designs of Beams and Groth the gas inlet and outlet pipes were part of the rotating shaft, with the almost inevitable difficulties of rotating seals and high power loss. In this latest machine, described by Bulang *et al.* (1960) and shown in Fig. 13, the gas inlet and outlet system used stationary pipes. The gas inlet was via a central stationary pipe extending right through the flexible rotating hollow shafts of the rotor. The top half of the pipe was used to feed the gas in, and the bottom half used as a pressure tapping to measure the axis pressure.

The gas extraction for the light and heavy fractions from the rotor ends utilized the stationary tube inside the flexible shafts shown in the figure. Attached to this stationary tube were two arms which extended outwards to a radius of 79 mm and which were bent around to face the gas stream. Following the terminology of the Steenbeck-Zippe machine described later, these are called scoops. The scoops utilized not only the high pressure at the increased radius but also the momentum of the rotating gas against the stationary scoop. The pressure given by this dynamic head was approximately equal to $\rho V^2/2$, greater than the static head at the scoop by a factor of $\hat{M}V^2/2RT$. In this relationship V is the gas velocity at the scoop radius and therefore slightly less than the peripheral speed of the rotor.

The main disadvantage, found in tests with isotopes of

TABLE VI. Dimensions of German and Russian rotors.

Type	Length (mm)	Diam. (mm)	Angular freq. (Hz)	Peripheral speed (m/sec)	Z/d	Thickness (mm)	Material
German							
UZ1	400	120			3.33		Bondur aluminum alloy
UZ111B	635	134	665	280	4.74	8	
ZG3	665	185	520	302	3.60		
ZG5	1130	185	520	302	6.11		
Russian							
Steenbeck	3000	60	1400	250	50	~1	aluminum 7075T6
Zippe	332	74	1500	350	4.48	~1	

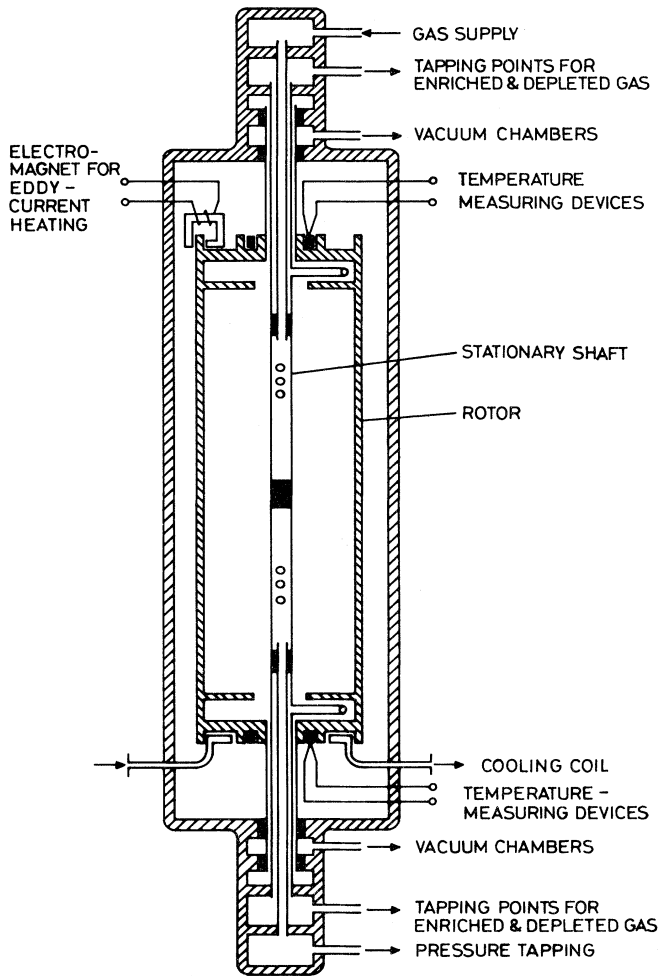


FIG. 13. Simplified diagram of ZG5 machine developed in Germany. This machine, the last developed by Groth, had a controlled method of setting up thermal countercurrent and used stationary scoops for gas extraction.

xenon, was that the scoops caused disturbances to the gas flows in the main countercurrent, reducing the separation. This was overcome by installing rotating partitions within the rotor, which were sealed at the perimeter but contained openings in the center of 40 mm diameter. The purpose of these partitions was to shield the gas in the main chamber of the rotor from the effects caused by the scoops in the end chambers. The experimental results with this arrangement showed that the separation was fully restored, although, for some reason not given, it was necessary to have a higher temperature difference between the ends than had been used in the earlier tests. This report in 1960 on the ZG5 machine was the last publication from the team initially set up during the war by Groth and Beyerle.

VII. PRINCIPLES OF BEARINGS

Before discussing the final machine in this review, that originally developed in the Soviet Union by Steenbeck and

Zippe, it is useful to consider the basic principles of bearings, another key item in the development of high-speed machinery. The development of bearings was an essential part of the industrial revolution of the last century, and several advanced bearing systems have been developed in the present century.

There are several ways of classifying bearing systems, but so far as rotating machinery is concerned they all have one main objective. This is to constrain the rotor to spin in some prescribed equilibrium position. To this end they behave like springs, giving a restoring force if the rotor is displaced from its equilibrium position, and the spring constant or stiffness of the bearing is one of the most important parameters in any classification system. This is mentioned because of the interesting fact that Beams and Groth chose one of the stiffest bearing systems available (hydrodynamic journal bearings) and Steenbeck and Zippe chose one of the weakest bearing systems available (the magnetic and pivot bearing), and that the physics of both bearing systems was developed at almost the same time at the end of the last century. The essentials of these two bearing systems are described in Appendix F, partly to give an insight into the principle of bearings and partly because these were the bearings actually used in the specific machines described in this review. There are several other bearing systems that could be used and have been used in high-speed centrifuges, but these are not relevant in the present review.

VIII. RUSSIAN MACHINES

These machines, initially developed in the Soviet Union during the period 1946–1954, are the most recent machines described in the literature. According to Zippe (1960), the team in the Soviet Union about 60 strong, was composed of both German and Russian workers, with Steenbeck directing the theoretical work and Zippe the mechanical and separation work. Initially they developed a supercritical centrifuge using short elements of tubes connected together by sylphons to give an overall length of 3 m and a ratio of length to diameter of 50:1. The tubes were made of aluminum alloy, giving a maximum peripheral speed of 250 m/sec, but few details of this supercritical centrifuge have been disclosed.

However, much more information is available on a small subcritical machine developed by the same group. This information is available because Zippe repeated his work during the period 1958–1960 at the University of Virginia and reported on the work in detail in 1960. Some of the mechanical work was also repeated at Degussa, Frankfurt, Germany, as described by Steenbeck, Zippe, and Scheffel (1957). The essential features of this subcritical machine are shown in Fig. 14, and the leading dimensions are given in Table VI. This machine, although still based on the De Laval self-balancing principle, differed in three respects from the Beams machine. These, of varying degrees of importance, were the bearing system, the rotor dynamics, and the hex feed and extraction system.

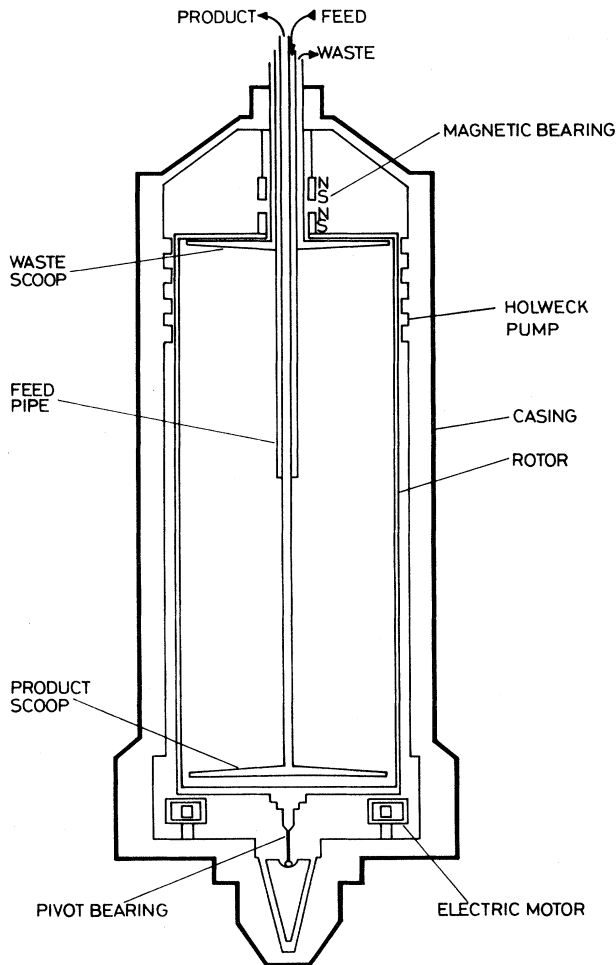


FIG. 14. Subcritical centrifuge supported by pivot and magnetic bearings. This machine, developed by Steenbeck and Zippe, used stationary feed and extraction systems and avoided the need for a complex array of seals.

A. Bearing system

As shown in Fig. 14, the rotor rests on a pivot bearing and is held upright by coaxial magnets. This magnetic bearing is also used to give an upward force to relieve the load on the bottom bearing, just as in the system described in Appendix F and originally developed by Evershed for his electricity meter. The rotor mass of 0.4 kg is about twice the Evershed limit, but Zippe used a larger pivot bearing and more powerful magnets. In retrospect it is surprising that magnetic bearings were not considered for the early American machines. There is a long history of development of magnetic bearings at the University of Virginia (see, for example, Beams, 1938, 1940), but there is no mention of their use in the history of the Manhattan Project. Instead the Virginia group chose the more robust conventional bearings, with a consequent power loss of about 2 kW per machine. This came about partly because in the original prewar work of Beams the power consumption was of no importance; the machine was designed as a one-off laboratory machine,

whose sole purpose was to obtain convection-free separation, and it was perhaps natural to follow this development when the work became part of the Manhattan Project.

Nevertheless, the decision by Steenbeck and Zippe to use the less robust combination of pivot and magnetic bearing enabled them to reduce the bearing power consumption by a factor of 1000 to only 2 or 3 W per machine.

B. Rotor dynamics

The rotor, made of aluminum alloy, was much thinner than those used by Beams and Groth, and was supported by the bearing system described above. The bearings used in Zippe's Virginian model were very asymmetrical, the bottom pivot assembly being very much stiffer than the top magnetic bearing. In such an asymmetrical system the low-speed cylindrical and conical modes of vibration shown in Fig. 2(a) are replaced by the two conical modes shown in Fig. 2(b), with the nodes at the bottom of the rotor and one-third down the rotor, respectively. These two conical modes of vibration were damped out using the tuned vibration absorber system. Both the top magnetic bearing and the bottom pivot bearing were flexibly mounted, with damping means between the moving part of the bearing and the machine frame. In the machine developed at Virginia the weak top magnetic bearing was tuned for the low-frequency precessions, and the much stiffer bottom pivot assembly was tuned for the high-frequency conical precession at operating speed.

At high speeds, after traversing the low-speed criticals, the rotor spun about its center of mass in much the same way as the Beams tubular rotor described earlier; also at these high speeds the gyroscopic torques took over, and the rotor precessions tended to the symmetrical modes with the frequencies given earlier. The amplitude of the low-speed criticals, as shown in Appendix B, can be derived from a Jeffcott-type analysis or by applying the energy equation to each mode separately.

C. The hex system

As described earlier, the hex was passed into, and taken out of the Beams centrifuges by means of hollow shafts attached to the rotor. This is satisfactory at low speeds, up to, say, 300 m/sec, when the pressure ratio from rotor wall to axis is only about 500 and the axis pressure is reasonably high. However, the Zippe machine at Virginia operated at 350 m/sec, with a pressure ratio of 5700. This gives too low an axis pressure for the gas to be extracted from the center. Because of this, and to allow the use of magnetic bearings, Steenbeck, Zippe, and Scheffel developed the system shown in Fig. 14. The feed and extraction system is a stationary assembly, entering the rotor through an opening in the magnets. The feed tube ends in the middle part of the rotor, while the extraction tubes terminate at opposite ends of the rotor and have, at

their extremities, hook-shaped Pitot tubes in a plane perpendicular to the axis of rotation. These scoops make use of the high impact pressure in the vicinity of the periphery, and, as described earlier for the ZG5 machine, the dynamic pressure head is greater than the static pressure by a factor of $\hat{M}V^2/2RT$, which is about ten at 350 m/sec. Detailed experimental results for various scoop arrangements are given by Zippe (1960).

The scoops used in the Groth ZG5 machine were shielded by baffles to prevent disturbances to the flow of gas in the main chamber of the centrifuge rotor. In the Zippe design, however, it was normal practice to shield only the product scoop assembly with a baffle, thereby preventing disturbance from only this scoop to the flow in the main hex chamber. The waste scoop was not shielded, and its disturbance was used to good effect to set up the axial countercurrent; at this unshielded scoop the gas is slowed down, caused to spiral inwards and then move axially, so inducing the required countercurrent.

Using this technique, Zippe performed a sequence of separation tests, the best of which gave an enrichment factor and a depletion factor of 1.09 at a throughput of 10.8 mg/sec UF_6 . This corresponds to a separative work output of 0.39 kg SW/yr, or a Dirac efficiency of 34%. In this test the rotor power loss was only 10 W, most of which was attributed by Zippe to drag on the scoops. Although this power loss was small, it had to be dissipated to the outer casing by radiation, and so the rotor ran a little hotter, relative to the casing, than the earlier Groth machines. This question of heat transfer is discussed in more detail in Appendix E.

IX. POSTSCRIPT

It is clear from this review that all three investigations before 1962 were highly successful projects, none more so than the Manhattan investigation. The conclusions of this project are listed by Beams (1975), and his last conclusion is the most important. To quote: "the limiting factor in the gas centrifuge was clearly the strength divided by the density of the rotor material. If this ratio could be increased, the effectiveness of the method would be increased accordingly." This consideration of the speed limitation of centrifuges is discussed last because it is the area of development in which the centrifuge specialist has least control, and yet it is this area in which the main advances of the centrifuge have been made. The development of materials of high specific strength has been almost entirely motivated by the requirements of the aerospace industry, and will be discussed briefly in this last section.

A. Stress analysis

There are two important requirements of the centrifuge rotor so far as stress analysis is concerned. These are that

- (a) the stress levels of the rotor components be no

greater than the acceptable working stress of the material of construction, and

- (b) the strain levels of the component be such that individual parts do not become loose at speed.

It is therefore necessary to perform a detailed stress analysis of any rotating system to ensure that these conditions are met. The theory of stress analysis forms part of the science of elasticity, probably the oldest discipline involved in the design of the centrifuge rotor. The full history of this science has been given by Timoshenko (1953), and so it is only necessary to give here the important features relevant to the stresses in rotating cylinders and discs, the two important components part of the centrifuge rotor.

The first more or less complete exposition of the stresses and strains in cylinders and discs was that of Chree (1891, 1982a, 1982b), following some earlier work by Maxwell (1850). The Chree stress analysis for a thin-walled cylinder is particularly important, giving the equation

$$\sigma = \rho V^2. \quad (21)$$

This equation, discussed at the beginning of the review, shows that the peripheral speed of a centrifuge is fixed only by the specific hoop strength of the material of construction. The Chree analysis also showed that the radial and axial strains depend on the specific modulus and the Poisson ratio of the material of construction according to the equations

$$\epsilon_r = \rho V^2 / E, \quad (22)$$

$$\epsilon_a = \nu \rho V^2 / E. \quad (23)$$

The analysis of discs is slightly more complicated, but the general result is that the stress levels of discs are much lower than those of tubes made of the same material and spinning at the same peripheral speed. This is because a disc can provide inward radial forces, like the spokes of a wheel, holding the whole disc in with a smaller overall strain relative to that of the tube given by Eq. (22). A summary of the exact Chree analysis is given in Appendix G, but the most important general result is that the maximum peripheral speed that can be attained by various tubes and discs is in every case limited by the strength-to-weight ratio of the material of construction.

B. High-strength materials

At the time of the Beams investigation the strongest available aluminum alloy had a working strength-to-weight ratio of 6.25×10^4 m²/sec²; this had about doubled by the time of the Zippe investigation at the University of Virginia. However, since that time there have been only modest increases in the strength of aluminum alloys. The major increases have been attained in the strength of titanium and steel alloys and in composite materials such as glass, carbon, and other fibers embedded in epoxy

resin. With these modern materials it is possible to more than double the rotor peripheral speed used by Beams. However, the application of these materials to centrifuge design will not be discussed here, since this is best left to a review of work from 1962 onwards. Suffice to say that the latest American centrifuge has an output of well over thirty times that of the best Manhattan machine. Thus instead of 30 000 machines being required for the wartime plant, the number now would be fewer than a thousand.

ACKNOWLEDGMENTS

The author wishes to thank Mr. A. Johnson, Director of the Enrichment Division of British Nuclear Fuels Limited, for permission to publish this article. The quotations from the paper by Evershed are courtesy of the Institution of Electrical Engineers, London.

APPENDIX A: THE ROSETTE ROTOR

Apart from the three major developments reviewed in the main text, there was a smaller project in the UK completed between 1946 and 1954 to assess the usefulness of the centrifuge relative to the UK diffusion plant. Most of the development work was done by the General Electric Company (GEC) on behalf of the United Kingdom Atomic Energy Authority. During this work a Beams-type centrifuge was fully developed, but one which ran at a much higher speed, necessitating the development of scoops for gas removal. None of this work has been published except for the novel design of rotor, which allowed operation at a speed fifty percent faster than in the equivalent projects in America and Germany.

As described earlier, the cylindrical rotors used by Beams and Groth were operated at speeds of up to about 300 m/sec, this limit being set by the specific strength of the highest-strength aluminum and steel alloys available during and immediately after the war. Boyland (1946) of GEC considered this speed to be too low for economic operation and developed the concept of the "rosette" rotor shown in Fig. 15. The principle of this design is that stresses are lower in surfaces of small radius of curvature than in surfaces of larger radius of curvature. In a conventional cylindrical rotor the curvature is fixed by the radius, which also determines the centrifugal force and the surface area. However, in the rosette design loops of small radius of curvature are supported at a distance from the axis of rotation several times their own radius, so giving an enhanced performance relative to a conventional cylinder. In the Boyland design, shown in Fig. 15, the shape and thickness of the supporting spokes are designed to give a uniform tensile strength in the material of 0.7×10^9 N/m² at 450 m/sec. A conventional rotor at this stress level would have a speed of only about 300 m/sec.

This fifty-percent or so increase in speed gives a potential increase in output, using the Dirac equation, by a factor of about 5. However, the volume taken up by the

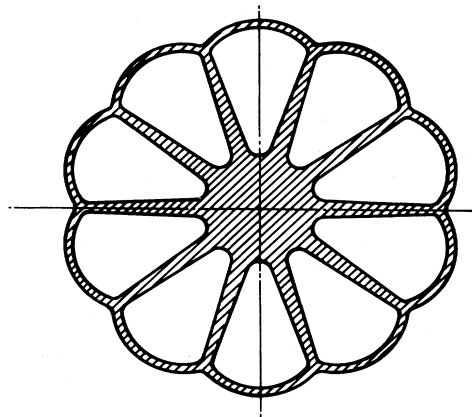
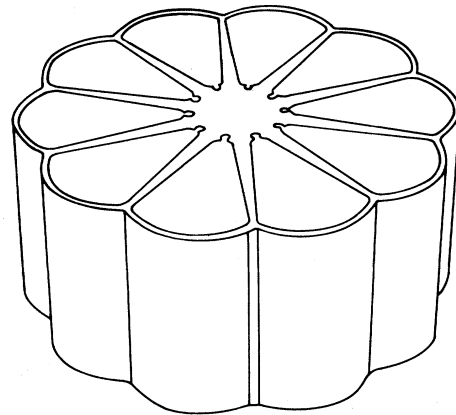


FIG. 15. The rosette rotor. Developed by Boyland for high-speed operation, approximately 50% faster than conventional cylinder.

spokes and the shape of the perimeter reduce this by factors of 0.92 and 0.64, respectively. Moreover, it is more difficult to achieve a high separation efficiency at the higher speed; Boyland achieved a maximum efficiency of only about 60%, compared with the 80% possible at the lower speed. These factors, taken together, give an overall improvement of about two for the rosette rotor at 450 m/sec compared with a cylinder at 300 m/sec. The possible improvement at other speeds requires individual calculation.

APPENDIX B: THE JEFFCOTT ANALYSIS OF SELF-BALANCING

1. Symmetrical rotor

The rotor and bearing system in the early machines of Beams and Groth were very nearly symmetrical. Therefore, the original analysis of self-balancing given by Jeffcott (1919) is immediately applicable to them. For example, for the system shown in Fig. 2(a), resolving the un-

balance in two planes gives for the symmetrical cylindrical whirl

$$\mathcal{M}\ddot{x} + 2\mu\dot{x} + 2Sx = \mathcal{M}\Delta\omega^2\sin\omega t \tag{B1}$$

and

$$\mathcal{M}\ddot{y} + 2\mu\dot{y} + 2Sy = \mathcal{M}\Delta\omega^2\cos\omega t . \tag{B2}$$

These equations can be solved independently (they are the standard equations for forced damped harmonic motion) or by using complex numbers, giving

$$\mathcal{M}\ddot{z} + 2\mu\dot{z} + 2Sz = \mathcal{M}\Delta\omega^2\exp(i\omega t) . \tag{B3}$$

The standard solution for these equations—see, for example, Wood (1940)—gives the amplitude and phase angle as

$$\frac{\mathcal{A}}{\Delta} = \frac{\omega^2}{[(\Omega_1^2 - \omega^2)^2 + (2\mu\omega/\mathcal{M})]^2} , \tag{B4}$$

$$\tan\delta = 2\mu\omega/\mathcal{M}(\Omega_1^2 - \omega^2) . \tag{B5}$$

Alternatively the sequence of events can be followed using a rotating vector method and studying the balance of forces on the rotor when it is spinning at speed ω , as shown in Fig. 16. The first diagram shows the necessary centripetal force required to keep the center of gravity of the rotor moving in the circular orbit. This force is from the center of gravity to the initial position at the origin. The second diagram shows the stiffness and damping forces available to provide this centripetal force. In this diagram all of the vectors are rotating at angular speed ω .

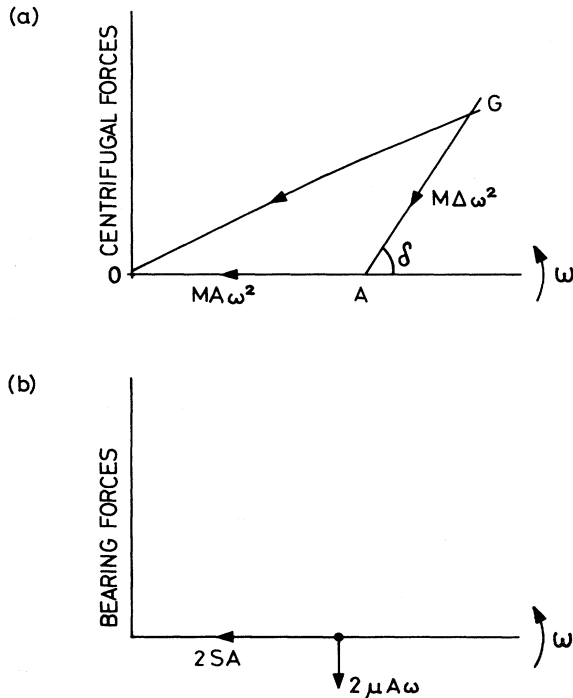


FIG. 16. Forces during self-balancing at cylindrical critical: (a) forces required to support shaft during whirl; (b) available bearing forces.

Resolving the forces gives

$$\mathcal{M}\mathcal{A}\omega^2 = 2S\mathcal{A} - \mathcal{M}\Delta\omega^2\cos\delta , \tag{B6}$$

$$2\mu\mathcal{A}\omega = \mathcal{M}\Delta\omega^2\sin\delta . \tag{B7}$$

Solving these equations again gives the standard solution for forced damped vibrations, which is plotted as amplitude versus speed in Fig. 17(a) and amplitude versus phase angle in Fig. 17(b). These curves show the gradual transition of the rotor from the low-speed condition of spinning about its geometric axis, through the critical condition of maximum amplitude, to the high-speed condition of spinning about its mass axis. The amplitude at the critical is approximately equal to

$$\mathcal{A}/\Delta = \mathcal{M}\Omega_1/2\mu . \tag{B8}$$

Exactly the same considerations apply to the conical mode, as shown, for example, by Allen, Stokes, and Whitley (1961). The Jeffcott equation for this mode, neglecting gyroscopic effects, is given by

$$I\ddot{\theta} + 2\mu I^2\dot{\theta} + 2SI^2\theta = Y\omega^2\exp(i\omega t) . \tag{B9}$$

The rotor amplitude $I\theta$, at the phase change position, is given by

$$\mathcal{B}/\Delta_1 = \mathcal{M}\Omega_2/4\mu . \tag{B10}$$

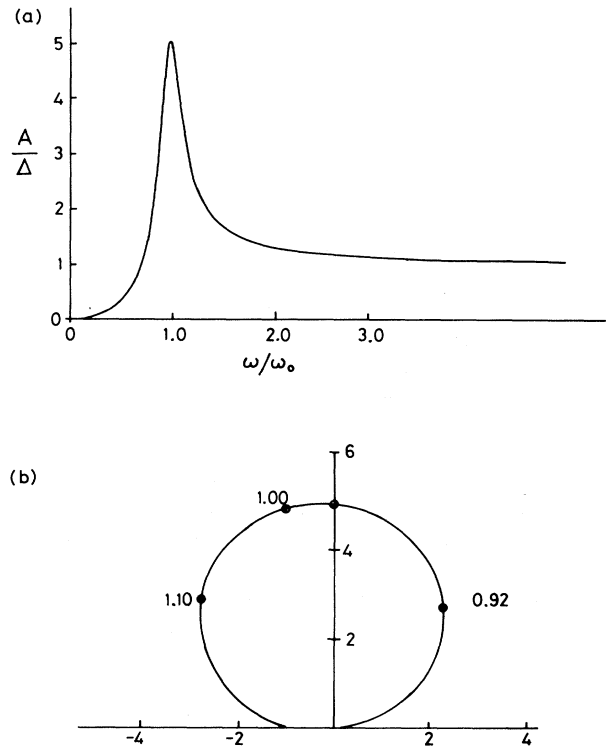


FIG. 17. Amplitude variations during self-balancing: (a) amplitude-frequency diagram showing high amplitude at critical; (b) polar diagram showing amplitude variation with phase change as speed increases (in the counterclockwise direction). The numbers 0.92, 1.0, and 1.10 define the speed relative to the critical speed.



FIG. 18. Amplitude variations during self-balancing: (a) amplitude-frequency diagram showing high amplitude at critical; (b) polar diagram showing amplitude variation with phase change as speed increases (in the counterclockwise direction). The numbers 0.92, 1.0, and 1.10 define the speed relative to the critical speed. The critical speed and the maximum amplitude are greater than given by Eqs. (13) and (16). These values apply when the phase angle is 90°.

TABLE VII. Mathematical model of dynamic absorbers. (In a standard absorber it is easiest to set the mass ratio g equal to m/M and work out the stiffnesses; in a bearing absorber one proceeds the opposite way. It is usually best to have a large mass ratio for the standard absorber and a small one for the bearing absorber.) (a) is for a standard vibration absorber while (b) is for a dynamic bearing absorber.

	(a)		(b)			
	Excitation constant	Excitation squared	Excitation squared	General	$k=0$	$S=0$
$\frac{k}{S} =$	$\frac{g}{(1+g)^2}$	$\frac{g}{1+g}$	$\frac{m}{M} =$	$\frac{Kk + KS + Sk}{(K+S)^2}$	$\frac{KS}{(K+S)^2}$	$\frac{k}{K}$
$\frac{\mu^2}{1.5Sm} =$	$\frac{g^2}{(1+g)^3}$	$\frac{2g^2}{(1+g)(2+g)}$	$\frac{\mu^2}{1.5Km} =$	$\frac{K}{K+S}$		1
$\frac{\mathcal{A}}{\Delta} =$	$\frac{(g+2)^{1/2}}{g^{1/2}}$	$\frac{2^{1/2}}{[g(1+g)]^{1/2}}$	$\frac{\mathcal{A}}{\Delta} =$	$1 + \frac{2g(K+S)^2}{K^2}$		$1 + 2g$

In this equation the couple out of balance is written as $\mathcal{M}\Delta_1/2$, which is equivalent to a center-of-mass shift of Δ_1 for the top half of the rotor and Δ_1 for the bottom half, but on the opposite side.

2. Asymmetrical rotor

The rotor and bearing system in the machines of Steenbeck and Zippe was asymmetrical—in fact, the machine was so asymmetrical that the two rigid-body criticals are as shown in Fig. 2(b). In this extreme case the two rigid-body resonances have modes at the bottom and one-third down the rotor, respectively. The completely general case has been treated by Timoshenko (1928), but in the extreme case of Fig. 2(b), the equivalent of the Jeffcott equations (B1) and (B9) can be written down immediately as

$$I_2\ddot{\theta} + \mu_2 L^2 \dot{\theta} + S_2 L^2 \theta = (XL/2 \pm Y)\omega^2 \exp(i\omega t), \quad (B11)$$

$$I_1\ddot{\theta} + \mu_1 (\frac{2}{3}L)^2 \dot{\theta} + S_1 (\frac{2}{3}L)\theta = (XL/6 \pm Y)\omega^2 \exp(i\omega t). \quad (B12)$$

The first gives a maximum amplitude at the top and the

second at the bottom, of values

$$\begin{aligned} \mathcal{C} &= (X/2 \pm Y/L)\Omega_3/\mu_2 \\ &= (\Delta/2 \pm \Delta_1/4)M\Omega_3/\mu_2 \end{aligned} \quad (B13)$$

and

$$\begin{aligned} \mathcal{D} &= (X/4 \pm 3Y/2L)\Omega_4/\mu_1 \\ &= (\Delta/4 \pm 3\Delta_1/8)\mathcal{M}\Omega_4/\mu_1. \end{aligned} \quad (B14)$$

Notice that in all cases the peak amplitude at the criticals is of the same form as and proportional to the nondimensional group $\mathcal{M}\Omega/\mu$.

APPENDIX C: METHODS OF DAMPING

De Laval in his self-balancing turbine used the stiffness of the shaft in series with the stiffness of the bearing film as the restoring force, and the damper force of the bearing film itself as the energy-absorbing force. His turbine is illustrated in Fig. 1(a) and is similar to the model treated by Jeffcott. The bearing and damping forces of hydrodynamic bearings are given in standard text books such as those of Pinkus and Sternlicht (1961) and Grassam and

Powell (1964). If the shaft is very flexible, most of the deflection in the self-balancing process occurs in the shaft, and the bearing movements are minimal—this is the De Laval case—but if the shaft is very stiff, most of the self-balancing occurs in the bearing film. Examples of this in gas bearing technology have been given by Fischer, Cherubim, and Decker (1959) and by Allen, Stokes, and Whitley (1961). However, this method was not used in the various centrifuges discussed in this review and will not be discussed further here.

The second method of providing damping, used in some centrifuges, derives from a most unexpected source which predates even the principle of self-balancing. Watts (1883), working for the Admiralty, developed a very simple method of reducing roll in warships and so increasing the stability of the gun platform. He adjusted the level of water in a tank, situated in the ship, to give it the same frequency as the rolling motion of the ship. Then, as the ship rolled, it set the water in resonant motion so dissipating energy and hence reducing the roll of the ship. Watts was able to reduce the roll of the 9200-ton warship "Inflexible" by a factor of 2 using only 50 tons of water. The important principle developed by Watts was to set the small mass into motion with an amplitude much greater than that of the main mass. The damping in the system is then very effective because the energy dissipated in a damper is proportional to the square of the velocity and hence the square of the displacement within the damper.

This device, sometimes called a tuned or dynamic vibration absorber, is now used extensively for vibration control, and a detailed method of optimization was given for it by Ormondroyd and Den Hartog in 1928. The dynamic model of this vibration absorber and the tuned bearing-damper system are compared in Table VII and Fig. 18. As can be seen, they are not quite identical, but the physical principles and the method of optimization of both devices are the same. Both employ Watts's approach, tuning the small mass so that it executes large movements, typically three or four times that of the main mass, and then optimizing the damping constant for maximum removal of energy. The optimum values given in Table VII are from the original paper by Ormondroyd and Den Hartog (1928), from Sauer and Garland (1948), and from Kirk and Gunter (1972). This last review paper is from the University of Virginia, where this system has been extensively developed for both gas and medical centrifuge application.

In the early American machines and in all of the German machines, a slightly different method was used in which the damping was provided by extra floating bearings which activated an external damping member. This third system, illustrated in Fig. 19, is very easy to use and allows the stiffness and damping to be set independently of each other, but it is wasteful in cost and energy usage, requiring two extra bearings per rotor. Strictly this method of providing damping is not so different from the other two, and all three methods can be derived from the general model shown in Table VII and Fig. 18.

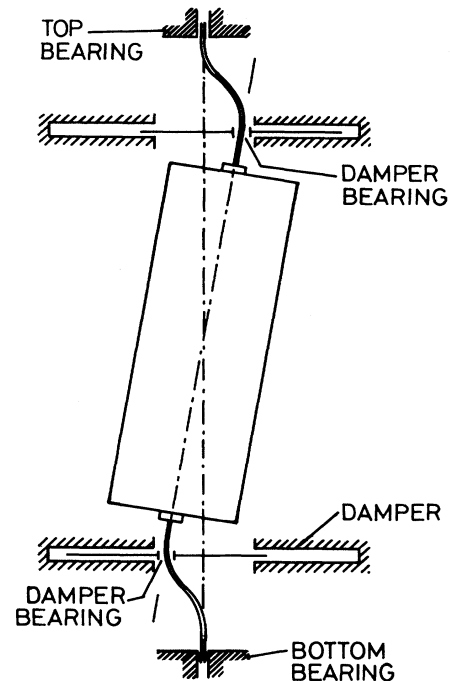


FIG. 19. Dynamic model showing separate damper. Two bearings at each end, one to support shaft and one to move and activate damper.

APPENDIX D: CONICAL MODE OF PRECESSION FOR SUBCRITICAL ROTORS

The main problems in spinning subcritical rotors are that

- (a) they have to traverse both the cylindrical and conical rigid-body criticals, usually at low speed, and
- (b) the rotors must be stable at operating speed, and therefore the cylindrical and conical natural modes must be well damped.

The difficulty is usually the conical mode at speed because of the normally large disparity in frequency between this mode and the others, making it necessary to design dampers to cover a wide frequency band. The relevant equations (12) and (14) for the conical frequencies are given in the main text; from these equations, the critical speeds and natural frequencies have been calculated and the results summarized in Table VIII. The calculations are given for various lengths of rotor and for three examples of bearing stiffness: a weak bearing typical of the Russian-type machine, a medium-stiff bearing system typical of the American/German machines, and a fairly stiff system typical of the original De Laval design. It is assumed that the stiffnesses are set in these three examples such that the cylindrical criticals are at 1%, 5% and 10% of the operating speed. This gives, from the self-balancing equation (18), reductions in bearing load of ten

TABLE VIII. Conical critical speed and conical natural frequencies of vibration (given as ratio to cylindrical critical speed in each case).

Length-diameter ratio	1.75	3.5	7.0	11.6	16.3
Polar/transverse inertia	0.68	0.23	0.063	0.023	0.012
Rotor mass kg	3.77	7.55	15.1	25	35
Stiffness for critical at 1% of full speed 10^3 N/m	4.60	9.20	18.4	30.5	42.8
		Cylindrical critical set at 1% of full speed			
Critical speed	2.50	1.85	1.76	1.74	1.74
Backward natural	0.03	0.12	0.43	0.91	1.23
Forward natural	68.5	23.1	6.73	3.25	2.42
		Cylindrical critical set at 5% of full speed			
Critical speed	2.50	1.85	1.76	1.74	1.74
Backward natural	0.14	0.52	1.19	1.50	1.61
Forward natural	13.8	5.12	2.45	1.97	1.85
		Cylindrical critical set at 10% of full speed			
Critical speed	2.50	1.85	1.76	1.74	1.74
Backward natural	0.28	0.84	1.42	1.61	1.67
Forward natural	7.12	3.15	2.05	1.84	1.79

thousand, four hundred, and one hundred, respectively. The values of mass and stiffness assumed in the table are those for an aluminum tube of 200 mm inside diameter and 6 mm thick, the nominal dimensions of the Westinghouse machines developed during the Manhattan Project.

It is clear from the table that to reduce the frequencies to reasonably low values, we must make the length-diameter ratio as large as possible, particularly if soft bearings are used. It is then easy to provide optimum damping because not only are the conical frequencies low, but also the amount of damping required is small, as shown by the energy equation (16). The shorter rotors can be operated more easily using the stiffer bearings, but then the radial load is high and the bearing may be unable to accept this higher load. As discussed earlier, the radial deflection at speed in a flexible bearing system is of the order of the center-of-mass shift Δ , and is independent of stiffness. In general, softer bearings have bigger clearances and allowable movements and can therefore accept this displacement in the bearing system more easily than stiff bearings.

This discussion of subcritical rotors is of course much simplified; more detailed information on the principles of subcritical rotors, including effects of asymmetric bearings, effect of end-mass, gyroscopic effects, rotor bow-balancing techniques, etc., is available in standard texts of machine design. Much useful information has been published by Anderson (1966) and Kelley (1963), but as pointed out by Anderson, the progression from principles to a workable machine is often as much an art as a science. "Years of accumulating information, developing design criteria, and correlating test data are required to advance a given high-speed centrifuge design to a firm basis." The complexity of a real design is apparent only from a detailed study of any one of the machines described in this

review, and a good example is the Westinghouse subcritical machine developed during the Manhattan program.

APPENDIX E: METHODS OF ACHIEVING CONVECTION-FREE OPERATION

1. Hydrogen stabilization

In the American and German projects undesirable temperature gradients were minimized by introducing hydrogen into the centrifuge casing. This hydrogen, although it helps to even out spurious temperature gradients, itself adds to the power usage due to drag on the rotor. To keep this extra power loss to a minimum it is necessary to reduce the pressure of hydrogen to a value which ensures laminar flow. Several measurements were made by Groth and his collaborators (1958) of the transition from laminar flow to turbulent flow, and their results are summarized in Table IX. Their results correspond to a Reynolds number at the transition of 350, rather higher than the value of $41(d/2h)^{1/2}$ or 150 quoted by Taylor (1923) for the onset of Taylor vortices. These results are not necessarily inconsistent because, as discussed by Schlichting

TABLE IX. Temperature stabilization of Groth machine.

Rotational speed	Hz	667	833	1000
Inside velocity	m/sec	281	351	421
Outside velocity	m/sec	314	393	471
Critical pressure	Pa	1890	1520	1270
Gas friction	W	55	84.4	124.3
ΔT	$^{\circ}\text{C}$	2.26	3.45	5.08

(1954), the flow can remain laminar well after the onset of Taylor vortices.

If flow conditions are laminar, then the power loss, which appears as heat, is given by the usual Petroff equation,

$$\mathcal{P} = \eta AV^2/h. \quad (\text{E1})$$

Half of this heat is given directly to the casing and the other half to the rotor. The temperature of the rotor therefore rises until the temperature difference is just enough for the hydrogen to conduct the heat to the outside casing. At equilibrium the temperature rise is given by the equation

$$\Delta T = \eta V^2/2\kappa = \hat{M}V^2/4C_v, \quad (\text{E2})$$

the latter equality being for a diatomic gas.⁵ Since all diatomic molecules have the same number of degrees of freedom and hence the same specific heat per mole, it is clear that hydrogen, with its small molecular weight, is the best gas to use for the purpose of temperature stabilization. The results given by Groth are summarized in Table IX.

The critical pressure listed in Table IX is the upper limit allowed before the flow becomes turbulent. If instead the pressure is set too low, the conditions tend to be molecular, and the efficiency of the heat transfer is diminished. The effect can easily be seen using the standard equations for molecular flow given by Kennard (1938). These are

$$\text{Heat flow/unit area} = p(1.2C_v/\hat{M})(\hat{M}/2\pi RT)^{1/2}\Delta T, \quad (\text{E3})$$

$$\text{Power/unit area} = p(\hat{M}/2\pi RT)^{1/2}V^2. \quad (\text{E4})$$

Strictly speaking, both these equations should be modified by factors to allow for the efficiency of energy and momentum transfer during individual molecular collisions—the accommodation coefficients. Assuming these coefficients are equal, the equations show that the temperature rise during molecular conditions is

$$\Delta T = \hat{M}V^2/2.4C_v, \quad (\text{E5})$$

rather worse than for the viscous condition. Moreover, if the working pressure is set at too low a value, the absolute value of the thermal conductivity decreases, and the hydrogen is less able to equalize out temperature gradients caused by spurious heat sources. To avoid these molecular conditions it is necessary to set the pressure higher than about 25 Pa (0.2 Torr), since at this pressure the mean free path is 0.05 mm, one-tenth of the gap.

The pressure can be set at any value between the upper and lower limits defining laminar conditions, and Groth normally set the pressure at about 400 Pa (3 Torr). Then, although the viscous drag due to the use of hydrogen was

significant—about 55 W at the lower speed—it was negligible compared with that of the bearings and seals, and the rotor temperature was only 2°C or 3°C hotter than the casing.

2. Vacuum operation

The main advantage of the centrifuge developed by the Russian team is that the power loss in the bearings is negligible and hence external spurious heat sources are eliminated. Moreover, the heat generated in the rotor itself, mainly from the scoop system, is only about 10–20 W, and this amount of heat can easily be transmitted from the rotor to the casing by radiation without the rotor's getting too hot. This means that it is practical to operate the rotor in a vacuum, which is the best method of eliminating unwanted heat sources and hence unwanted convection.

However, in this type of centrifuge, hex can leak out of the rotor through the annular gap between the stationary feed system and the top end cap. It is therefore difficult to ensure that the cylindrical part of the rotor runs in a high vacuum. The Russian team solved this problem by using the outer surface of the rotor as part of a molecular pump, arranging the direction of pumping such that the hex was confined to the top end of the machine, with only a minute partial pressure outside the rotor.

Molecular pumps were first developed by Gaede (1913), before the advent of the diffusion pump, and then developed for cylindrical surfaces by Holweck (1923) and for discs by Siegbahn (1940). The pump shown in Fig. 14 is a Holweck cylindrical type, with the spiral grooves cut into the inside of the stationary vacuum surface, and the outside of the centrifuge rotor providing the rotating part of the pump.

If the pressure is sufficiently low for conditions to be molecular, then these pumps have a pressure ratio which depends on the ratio of rotor velocity to molecular velocity, giving, for a simple linear slot,

$$\ln(p_2/p_1) = 2\hat{L}V/3h\beta. \quad (\text{E6})$$

As can be seen, in contradistinction to the diffusion pump, these pumps are far more effective for the slower-moving heavy molecules, a decided advantage in this application. If the pressure is higher, so that the flow is laminar, the pump gives a constant pressure difference

$$\Delta p = 6\eta V\hat{L}/h^2. \quad (\text{E7})$$

These Gaede equations apply only when the flow and pressure change are in the direction of movement, as in his pumps. In the case of the Holweck and Siegbahn pumps, the flow and pressure change are at right angles to the rotor movement, and for these pumps optimized groove patterns must be used, as described, for example, by Whipple (1951) and Sickafus, Nelson, and Lowry (1961). In general the pressure ratios at these optimum values are much lower than those given by Eqs. (E6) and (E7), and the right-hand side of these equations must be

⁵From Kennard (1938). $\hat{M}\kappa/\eta C_v = (9\gamma - 5)/4 \sim 2$ for diatomic molecules.

multiplied by about 0.1.

Zippe (1960) has confirmed the validity of these theories for molecular pumps, showing it is easy with a Holweck pump to get pressure ratios for hex of 10^4 or more. This, together with the low axis pressure of a high-speed centrifuge, effectively eliminates any power loss due to gas friction on the outside of the rotor. For example, the axis pressure for the Zippe centrifuge at 350 m/sec is a few pascals, so the partial pressure of UF_6 in the rotor casing will be of the order of 10^{-4} Pa. At this low pressure the mean free path for UF_6 is about 20 m, so the flow is in the molecular regime. At this pressure, using Eq. (E4), it can be shown that the power loss due to drag on the rotor of the Zippe machine is less than 0.1 W. Thus, since there is negligible power loss both in the bearings and on the outside of the rotor, there is no possibility of undesirable convection currents to disturb the desired countercurrents.

APPENDIX F: BEARING SYSTEMS

1. Hydrodynamic bearings

The original experiment showing the pressure rise which occurs in a hydrodynamic journal bearing and which lifts rotors away from contact with the bearing surface was made in 1883. Towers, investigating locomotive bearings, was puzzled by the constant ejection of a plug which blocked up a hole in the bearing. The moment he attached a pressure gauge and observed the pressure rise in the bearing, the principle of hydrodynamic lubrication became clear, and it was not long before Reynolds (1886) had worked out the theory of the effect. The principle is that between the two eccentric cylinders of the rotor and the journal bearing there is a converging gap—a “wedge”—into which lubricant is pumped by the relatively rotating surfaces. This produces a pressure rise sufficient to lift the rotor away from the bearing. The exact pressure rise which occurs for a given bearing configuration involves solving the Reynolds equation, and the solution for a long journal bearing was first given by Sommerfeld (1904).

However, it is not necessary to consider bearing theory in detail, since a cursory examination of a stepped bearing is sufficient to demonstrate the “wedge” effect in bearings and give the relationship between load capacity and power consumption. The effect is indicated in Fig. 20. The lubricant is dragged along by the moving bearing surface in the direction of the converging gap at a mean velocity of $U/2$. Since this flow is too great to get out at the end of the converging gap, the pressure rises, inhibiting the entry flow and helping the exit flow so that they are equal. Thus at equilibrium the pressure rise is a balance between viscous drag flow, proportional to the gap h , and the opposing laminar or Poiseuille flow, which is proportional to $1/h^3$. This gives a resulting pressure rise and load capacity proportional to $1/h^2$.

On the other hand, the frictional power loss given by

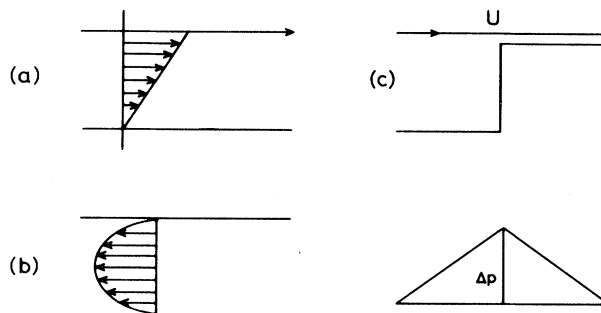


FIG. 20. Principle of self-acting bearing: (a) flow into bearing caused by viscous drag; (b) opposing Poiseuille flow caused by pressure buildup in the converging gap; (c) pressure rise at equilibrium.

Petroff's equation (E1) is proportional to only $1/h$, so that the ratio of power to load is proportional to the gap. For example, the power-to-load ratio for the infinitely long journal bearing, at an eccentricity of 0.5, is given by

$$\mathcal{P}/W = \omega h / 6 . \quad (\text{F1})$$

This equation is derived from the Sommerfeld solution for a long bearing. Similarly for a short journal bearing,⁶ described by Dubois and Ocvirk (1953), the ratio is

$$\mathcal{P}/W = 4\omega h / (\mathcal{L}/D)^2 . \quad (\text{F2})$$

This dimensional-type equation is fairly general; a similar equation exists for thrust bearings. For example, the constant in Eq. (F1) is 2.34 instead of 0.16 for an optimized hydrodynamic spiral groove bearing (see Whitley, 1967), and is 1.75 for an optimized hydrostatic bearing. This latter figure is easily derived by the methods given by Fuller (1956), assuming the step extends to half the radius of the bearing.

A similar relationship can be simply deduced for the other important parameter, the bearing stiffness. If the load capacity is proportional to $1/h$, it follows by differentiation that

$$S = -W/h \quad (\text{F3})$$

and therefore

$$\mathcal{P}/S \sim \omega h^2 . \quad (\text{F4})$$

These nondimensional equations are important in showing that, for the lowest power consumption, it is better to use precision bearings working at a small gap rather than large-clearance conventional bearings.

The failure to develop such optimized but conventional bearings was one of the main problems with the Beams and Groth machines. These machines were developed under wartime conditions, and the decision was taken to use robust journal bearings on the outside of the rotating

⁶In these equations no account is taken of the attitude angle, i.e., the angle between the load and the displacement.

gas pipes, along with the complex rotating seals they made necessary. This sequence of design philosophy leads almost inevitably to a high power consumption, with the consequent danger of creating unwanted convective currents in the gas in the centrifuge rotor, so destroying the separating effect. Then, to prevent these convection currents, it is necessary to introduce hydrogen at low pressure into the centrifuge casing to thermally stabilize the machine, and this consumes more power again.

2. The Evershed bearings

In retrospect, the design philosophy leading to such high power loss in the American and German centrifuges should not have been inevitable because the problem of making precision bearings of low power consumption for instruments, etc., was not itself new; the same problem had to be solved in the last decade of the 19th century in the design of electricity meters for the emerging electricity industry. In this application minimum friction is essential. However, these meters are essentially low-speed devices, for which hydrodynamic bearings are not appropriate. Instead pivot and magnetic bearings were developed. Figure 21 shows the system designed by Evershed (1900).

In this arrangement the pivot bearing at the bottom consisted of an accurately rounded shaft which ran in a spherical cup of radius of curvature rather larger than that of the shaft end. The earlier rule relating power to load capacity also applies to these bearings. This can be seen by examining an annular shaft running on a plane surface as in Fig. 22. Here

$$\mathcal{P} / W = f \omega b, \tag{F5}$$

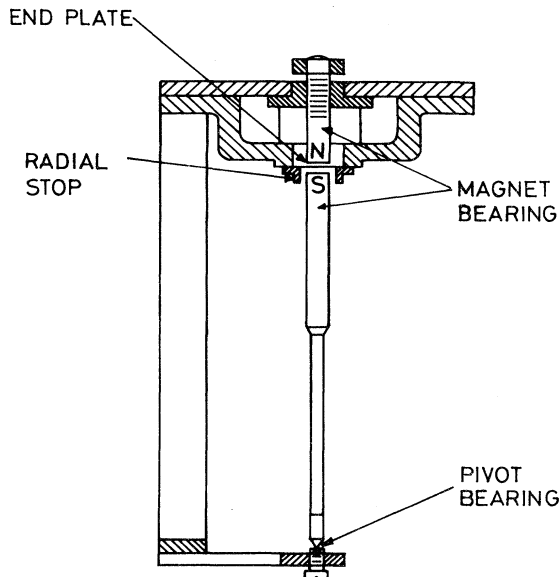


FIG. 21. Details of Evershed's magnetic suspension in a frictionless meter. The first practical pivot-magnetic bearing system developed for electricity meters (1900).

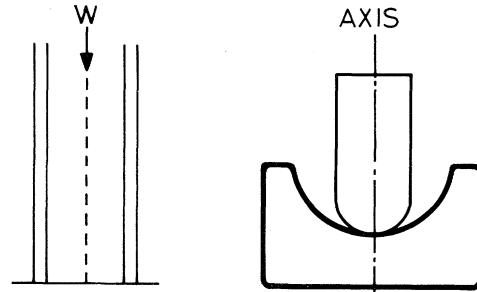


FIG. 22. Power loss in pivot bearings: (a) annular contact, $\mathcal{P} = f \omega W b$; (b) elastic contact, $\hat{\mathcal{P}} = (3\pi/16) f \omega W b$; (c) wearing contact, $\hat{\mathcal{P}} = \frac{1}{2} f \omega W b$.

where the friction coefficient is about 0.1 for lubricated bearings (see, for example, Shotter and Tagg, 1960).

It can be seen from Eq. (F5) that to reduce the power consumption it is necessary to minimize both the load and the radius of contact of the two surfaces. These two self-evident truths were the basis of the work of Evershed in his search for a "frictionless" electricity meter in the last ten years of the nineteenth century.

a. Pivot bearing

First consider the Evershed pivot bearing. This comprises a hard steel pin, rounded to a diameter of 0.25–0.35 mm, sitting in a cup of 1–2 mm diameter. This type of bearing, sometimes called a jewel bearing because the cup is often made of sapphire or diamond, is now used in a variety of sizes, from small watch bearings to large compass bearings. There is now an extensive literature on these bearings, e.g., Grodzinski (1942) on their manufacture, Stott (1931) on their wear characteristics, Shotter and Tagg (1960) and Kauzlarich, Wavrik, and Friedericy (1967) on general principles. Essentially the earlier theory of Shotter and Tagg is an elastic theory, while the later theory developed at the University of Virginia is a wear theory. Both theories, however, confirm the relationship between the power and load given by Eq. (F5), with a correction factor of $3\pi/16$ on the elastic hypothesis and 0.5 on the wear hypothesis.

One of the earliest to write on the elastic theory, Hertz (1896), showed that the radius of elastic contact between two spherical surfaces is given by

$$b^3 = 3W\Psi r_1 r_2 / 16(r_1 - r_2), \tag{F6}$$

where Ψ , a modified elastic constant, is equal to $0.16 \times 10^{-12} \text{ m}^2/\text{N}$ for steel. The specific load Q between the two surfaces is a maximum at the center of the circle of contact and zero at the outside, according to the equation

$$Q = 1.5Q_1(1 - r^2/b^2)^{1/2}. \tag{F7}$$

With the use of this equation it is easy to ensure that the peak pressure between the contacting surfaces is within acceptable limits for the materials of construction and to

show that the power loss is just $3\pi/16$ of that given by Eq. (F5).

The wear theory of the pivot bearing is more difficult, particularly in the prediction of long-term performance. A lubricated pivot bearing has a friction factor of about 0.1; this is typical of boundary lubrication, and consequently some wear is to be expected. It is assumed by Kauzlarich *et al.* (1967) that the wear will follow the law given by Archard and Hirst (1956), i.e., that the volume of material removed at any given radius is proportional to the applied load and the distance traveled. It is clear from this law that, if wear occurs, the load distribution must change such that the specific load varies inversely as the circumferential velocity at each point of contact—otherwise the pivot would not wear down uniformly. This gives

$$Q = Q_1 b / 2r . \quad (\text{F8})$$

Clearly at the center of the area of contact the peripheral velocity is zero and the load, from Eq. (F8), is infinity. In fact, of course, the central zone of the area of contact deforms plastically. If this small plastic zone is neglected, it is easy to show that the power loss is one-half of that given by Eq. (F5).

According to Kauzlarich *et al.* (1967), the load variation changes from the elastic condition to the wear condition after only about 100 revolutions. Thereafter, at least in principle, the friction should gradually increase as the area of contact increases. However, the problem becomes complicated by the presence of wear debris between the contacting surfaces and the possible onset of abrasive wear. The main experimental evidence available is that of Shotter and Tagg (1960), who investigated the effect of lubrication and the pressure between the bearing surfaces. They also did important work showing that with sapphire cups it was best to have the optic axis of the sapphire at right angles to the axial load. In the experiments of Shotter and Tagg, the maximum number of revolutions tested was about 2×10^9 , which, while sufficient for electricity meters, corresponds to only about 20 days of operation for the centrifuges described in this review.

The other important bearing parameter required is the radial stiffness. If the spherically shaped pivot were to slide up an inclined plane, the restoring force would be constant. However, as it slides up the gradually increasing slope of the spherical cup the restoring force increases linearly with radial displacement, thus giving a stiffness

$$S = W / (r_1 - r_2) . \quad (\text{F9})$$

For most pivot bearings, the radial and axial load capacities are approximately equal, so that Eq. (F9) is effectively of the same form as Eq. (F3) for journal bearings. More exact calculations are given by Shotter and Tagg (1960).

In these theories it is assumed that the area of contact between the surfaces of the pivot and cup is small, and therefore entails a very high specific load and elastic deformation between the contacting surfaces. However, from Eq. (F9), we see that it is necessary to decrease the

difference in the radii of the pivot and cup in order to increase the radial stiffness of the bearing. Then, from Eq. (F6), the area of contact increases, and these conditions eventually do not apply. In the limit, as the difference in radii tends to zero, the bearing merges into a hydrodynamic bearing, and the theory becomes more complex. The cylindrical part of the pivot bearing begins to behave as a conventional journal bearing, setting up a pressure difference around its periphery. The oil in the high-pressure zone is pushed out axially, some up and out through the equatorial part of the bearing, but some also down into the crescent shape under the spherical tip, giving some axial lift. The theory of this effect is given by Shaw and Strang (1948), with more recent work by Pan (1962).

b. Magnetic bearing

Perhaps the most important results from the above discussion are the stiffness equations (F3) and (F9). These equations are dimensionally correct and apply, as well, to passive magnetic bearings. They give the radial stiffness (apart from a constant) as the radial load divided by radial gap. Thus for a given load capacity the stiffness is inversely proportional to the radial gap. Typically the radial gap of a small journal bearing is about $25 \mu\text{m}$, that of a pivot bearing $250 \mu\text{m}$, and that of a magnetic bearing 2.5 mm. Therefore, for equivalent bearings, each designed to carry, say, a radial load of 10 N, the relative stiffnesses would be 400, 40, and 4 N/mm.

This last stiffness is extremely low, and therefore magnetic bearings, at least on first acquaintance, may seem unusual. Most people's concepts of a bearing are that it can carry a load of hundreds of newtons force, with a clearance of about $25 \mu\text{m}$, and, if it is overloaded, it hits metal to metal and is destroyed. A typical magnetic bearing may carry a load of only say 5 N with an acceptable radial movement of 0.5 mm, but then if it is overloaded it falls out of the magnetic field and, if there is no physical restraint, the rotor it supports will fall over. Magnetic bearings can be categorized as being of very small load capacity, large clearance, and low stiffness. They do, however, have two major advantages: they have almost zero power loss, and they can work in a vacuum.

The description given here is from an early paper by Evershed (1900), in which he developed the system shown in Fig. 21 which has a pivot bearing at the bottom and a magnetic bearing at the top. Evershed discussed these two bearings as a total system. He recognized that for minimum power consumption of the bottom bearing it was necessary to relieve the applied load as much as possible. This, as described earlier, has the effect of reducing not only the load, but also the radius of contact. Thus the Evershed magnetic bearing not only gave the required radial stiffness at the top of the rotor without itself causing any power loss, but it also gave an upward attractive force, thereby improving the performance of the bottom bearing.

There is, however, a danger in using the upward attrac-

tive force of a passive⁷ radial magnetic bearing, because in this direction the bearing is unstable. For example, if the rotor in Fig. 21 is moved upwards in the axial direction, the force between the magnets increases. If the axial lift increases too much it can lead to contact and failure. If the upward force follows an inverse square law of attraction, then it follows by differentiation that there is a negative stiffness in the axial direction of $2W/h$.

The instability of magnetic bearings at right angles to the direction of stability is a consequence of a basic law of magnetic bearings. This law, enshrined as Earnshaw's theorem (1839), and given by Maxwell (1881), is that it is impossible for a pole placed in a static field of force to have a position of stable equilibrium when an inverse square law relates force and distance. From this it follows that it is impossible to achieve magnetic levitation, stable in three dimensions, using only static magnetic fields. A corollary of this, important in the present context, is that in a radial magnetic bearing the stabilizing stiffness S in the radial direction must be less than half the negative destabilizing stiffness; this incidentally confirms the relationship between stiffness, load, and gap.

In 1900 Evershed discussed these problems as follows (he called his magnetic bearing a magnetic pivot and his pivot bearing a step bearing):

"A magnetic pivot of this type may easily be made to support a weight of from 100 to 200 grammes. Of course the position of the axle is one of unstable equilibrium in a vertical direction, the magnetic attraction increasing rapidly if the axle rises towards the supporting pole. But if means are adopted to confine the possible travel of the axle within narrow limits, it will run with very little pressure on the step bearing."

The end plate shown in Fig. 21 is in fact to stop the rotor from jumping. If the meter rotor gets a jolt and lifts off the pivot bearing, it will hit the end plate and fall back again.

As discussed above, by reducing the force on the pivot bearing, one can reduce the wear and power consumption considerably. The power consumption of the magnetic bearing itself is negligible, providing it is symmetrical about the axis to avoid eddy current losses. Thus, quoting again from the Evershed paper,

"We thus arrive at an essential principle for magnetic suspension of meter axles: the induction density in the magnetic devices used for support must remain absolutely constant during rotation of the axle. This at once disposes of unsymmetrical bipolar arrangements; nothing of the nature of the two poles attracting a piece of iron will serve. To secure uniform induction density in the rotating part of the magnetic circuit, the attracting pole must be a figure of revolution, with its axis coincident with the axis of rotation. As an example, the attracting pole might be a ring concentric with the axle."

⁷There are also "active" magnetic bearings using electromagnets with feedback control loops. These, not discussed here, can take much bigger loads—see Geary (1964).

In fact, the centrifuge described by Steenbeck and Zippe uses a magnetic bearing which is made of such concentric annular rings, as shown in Fig. 23.

Although magnetic bearings are now well established and in considerable use—over 300 papers on them are listed by Geary (1964)—a theoretical assessment is not yet available. The designs usually use semiempirical methods such as those described by Milligan and Green (1953). The problem is that it is difficult to calculate the magnetic force, given by the standard equation (Rotor, 1941)

$$F = \frac{1}{2}(mmf)^2 dq/dz,$$

where the permeance q is the inverse of magnetic reluctance. To determine the reluctance or permeance involves solving the magnetic field equation for the prescribed boundary conditions defined by the magnet surfaces. This in itself is a sufficiently difficult problem to solve, particularly since most magnets in bearings have sharp corners and hence saturation effects can occur. However, to determine the stiffness of a magnetic bearing it is necessary not only to calculate the permeance, but also to calculate the second derivative of permeance with distance, and this is a virtually intractable problem without the use of large computers.

Further details of the theory of magnetic bearings are beyond the scope of this paper, but this short description of both pivot and magnetic bearings shows that very little in modern machine design is truly novel. Even Evershed, who did most of his work between 1891 and 1900, found he was not alone in working on magnetic and pivot bearings. In fact, at the meeting in 1900 other workers claimed precedence over his invention, and T. Lockwood, President of the American Institute of Electrical Engineers, reminded the meeting of the quotation,

"People of old times had very little honesty: they have stolen all our best inventions."

This quotation seems particularly apt when one studies the work of Steenbeck, Zippe, and Scheffel, who developed their centrifuge initially in the Soviet Union and later in Germany and America. Their bearing system, shown in Fig. 14, is virtually a replica of the first Evershed design.

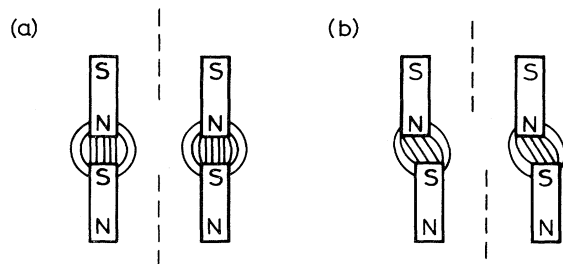


FIG. 23. Enlarged view of Evershed's top magnetic bearing: (a) equilibrium condition, attractive force W , attractive instability $dW/dh = 2W/h$; (b) displaced condition, radial stiffness $S \leq \frac{1}{2} dW/dh \leq W/h$.

TABLE X. Stresses and strains in discs (values for plain discs divided by ρV^2).

		Inner radius	Outer radius
Disc with central hole	Radial stress	0	0
	Circumferential stress	$(3 + \nu)/4$	$(1 - \nu)/4$
	Circumferential strain		$(1 - \nu)/4E$
Solid disc	Radial stress	$(3 + \nu)/8$	0
	Circumferential stress	$(3 + \nu)/8$	$(1 - \nu)/4$
	Circumferential strain		$(1 - \nu)/4E$
De Laval disc	Radial stress	σ	σ
	Circumferential stress	σ	σ
	Circumferential strain		$(1 - \nu)\sigma/E$

APPENDIX G: STRESS ANALYSIS OF DISCS

One of the earliest satisfactory expositions of the theory of rotating discs was that of James Clerk Maxwell (1850), who completed his study before he was 19 years old. However, the best early papers on the stress in both discs and cylinders are those by Chree (1891, 1892a, 1892b), and his theory is still used today. Chree was a distinguished authority on terrestrial magnetism and atmospheric electricity and was Superintendent of Kew Observatory for 32 years. He was also a past President of the Physical Society and the Royal Meteorological Society. This is mentioned to show how the theory of elasticity and mechanics was considered the proper province of distinguished scientists during the industrial revolution.

The Chree analysis for a thin-walled cylinder is given in the text, and his Eq. (2) is probably the best known result in the mechanical theory of centrifuges. This result shows that the maximum peripheral speed of a spinning rotor depends only on the specific strength of the material of construction, i.e., its working strength divided by its density. Providing the cylinder is thin, it does not depend on its thickness. (If the thickness and hence mass is doubled, the hoop force or tension is doubled, but the hoop stress is unaltered.)

The analysis for discs is more complicated, but the general result is that stress levels in discs are much lower than in thin cylinders. This is because a disc can provide inward radial forces, so keeping the disc to a small overall strain. For example, for a plain disc the circumferential strain and stress at the perimeter is only about $\frac{1}{6}$ of that of a thin cylinder. Although both the radial and circumferential stresses increase as one moves towards the center, their maximum and equal values at the center are still less than half that of the hoop stress in a thin cylinder spinning at the same peripheral speed. The exact values are listed in Table X. For a disc with a small central hole, the radial stress at the center falls to zero, and this weakening of the radial restraint causes the inner tangential stress to exactly double.

This Chree analysis for discs with and without a center hole gives only the values of the radial and hoop stresses; before application to design, it is necessary to combine these stresses in some way. This has been the subject of

considerable debate (see, for example, Juvinal, 1967), but the generally preferred method for ductile materials is the one originally proposed by Maxwell (1856), which has to do with the maximum distortion energy that a material can take up. With the use of the Maxwell criteria it is easy to work out a uniaxial stress equivalent to the "sum" of the two stresses in the disc, giving

$$\sigma_e^2 = \sigma_r^2 + \sigma_h^2 - \sigma_r \sigma_h . \quad (G1)$$

From this and the Chree analysis it follows that a disc with a central hole can spin about 10% faster than an equivalent tube, and a solid disc about 55% faster.

However, a solid flat disc is not the optimum shape for maximum speed. The outer regions of the disc are not stressed to the maximum possible value, and therefore this region should be thinned down. The best shape for a disc which carries a radial load was devised by Smith (1896), one of De Laval's research staff. In this model the thickness is varied to maintain the radial and tensile stresses at their maximum values throughout the disc, so that every part of the material contributes to the strength of the disc. These discs are usually called De Laval discs. The shape, as indicated in Fig. 1, is exponential, according to the equation

$$t = t_m \exp(-\rho \omega^2 r^2 / 2\sigma) . \quad (G2)$$

Rearranging gives the maximum speed of operation of a De Laval disc as

$$V_d^2 = 2V^2 \ln \lambda . \quad (G3)$$

A typical De Laval disc of thickness ratio from center to edge of, say, $\lambda = 5$ could thus spin faster than the equivalent tube by a factor of 1.8. In this design of turbine disc there is an outward radial stress (equal to the working stress σ) at the perimeter of the disc, and the whole disc strains radially by $(1 - \nu)\sigma/E$. Without this large outward stress the disc could spin even faster.

REFERENCES

- Allen, D. S., P. J. Stokes, and S. Whitley, 1961, "The performance of externally pressurised bearings using simple orifice restrictors," ASLE Trans. 4, 181.

- Anderson, N. G., 1966, "The development of zonal centrifuges and ancillary systems for tissue fractionation and analysis," National Cancer Institute Monograph 21, US Department of Health, Education, and Welfare, Bethesda, Maryland, USA.
- Archard, J. F., and W. Hirst, 1956, "The wear of metals under unlubricated conditions," *Proc. R. Soc. London, Ser. A* **236**, 397.
- Arnold, R. N., and L. Maunder, 1961, *Gyrodynamics and its Engineering Applications* (Academic, New York/London).
- Beams, J. W., 1936, "The separation of isotopes by centrifuging," *Phys. Rev.* **50**, 491.
- Beams, J. W., 1937, "High rotational speeds," *J. Appl. Phys.* **8**, 795.
- Beams, J. W., 1938, "Tubular vacuum-type centrifuge," *Rev. Sci. Instrum.* **9**, 413.
- Beams, J. W., 1975, "Early history of the gas centrifuge work in the USA," University of Virginia Report NP-20433.
- Beams, J. W., and C. Skarstrom, 1939, "The concentration of isotopes by the evaporative centrifuge method," *Phys. Rev.* **56**, 266.
- Bishop, R. E. D., and D. C. Johnson, 1960, *The Mechanics of Vibration* (Cambridge University, Cambridge).
- Boyland, D. A., 1946, "Improvements in or relating to Hollow Rotors and Centrifuges," British Patent 608,692.
- Bulang, W., W. Groth, I. Jordan, W. Kolbe, E. Nann, and K. H. Welge, 1960, "The separation potential of thermally driven countercurrent gas centrifuges," *Z. Phys. Chem. (Frankfurt am Main) New Series* **24**, 249. University of Virginia Report EP-4422-117-60 U, AEC translation No. 4249.
- Chree, C., 1889, "A solution of the equations for the equilibrium of the elastic solids having an axis of material symmetry, and its application to rotating spheroids," *Proc. Cambridge Philos. Soc.* **7**, 31.
- Chree, C., 1891, "On thin rotating isotropic disks," *Proc. Cambridge Philos. Soc.* **7**, 201.
- Chree, C., 1892a, "Long rotating circular cylinders," *Proc. Cambridge Philos. Soc.* **7**, 283.
- Chree, C., 1892b, "Changes in the dimensions of elastic solids due to given systems of forces," *Proc. Cambridge Philos. Soc.* **7**, 319.
- Chree, C., 1904, "The whirling and transverse vibrations of rotating shafts," *Philos. Mag. Series 6*, **7**, 504.
- Cohen, K., 1951, *The Theory of Isotope Separation as Applied to the Large Scale Production of U²³⁵* (McGraw-Hill, New York).
- De Laval, G., 1879, in *Gustaf De Laval 1845–1913, De Hoga Hastigheternas Man*, by T. Althin (Swedish De Laval Steam Co., Stockholm, Sweden).
- Den Hartog, J., 1934, *Mechanical Vibrations* (McGraw-Hill, New York).
- Dubois, G. B., and F. W. Ocvirk, 1953, "Analytical derivation and experimental evaluation of short bearing approximation for full journal bearings," National Advisory Committee for Aeronautics, Report No. 1157.
- Dunkerley, S., 1894, "On the whirling and vibration of shafts," *Philos. Trans. R. Soc. London* **185**, 279.
- Earnshaw, S., 1839, "On the nature of molecular forces which regulate the constitution of the luminiferous ether," not published until 1842, *Trans. Cambridge Philos. Soc.* **7**, 97.
- Evershed, S., 1900, "A frictionless motor meter," *J. Inst. Electr. Eng.* [1889–1940] **29**, No. 146, 743.
- Fischer, G. K., J. L. Cherubin, and O. Decker, 1959, "Some static and dynamic characteristics of high speed shaft systems operating with gas lubricated bearings," *First International Symposium of Gas Lubricated Bearings*, edited by D. D. Fuller (Office of Naval Research, Department of the Navy, Washington, D.C.), p. 383.
- Fuller, D. D., 1956, *Theory and Practice of Lubrication for Engineers* (Wiley, New York).
- Gaede, W., 1913, "The molecular air pump," *Ann. Phys. (Leipzig)* **41**, 337.
- Geary, P. J., 1964, "Magnetic and electric suspensions," SIRA Report R314, British Scientific Instrument Research Association, Kent, England.
- Grassam, N. S., and P. J. Powell, 1964, *Gas-Lubricated Bearings* (Butterworths, London).
- Grodzinski, P., 1942, *Diamond and Gem Stone Industrial Production* (N.A.G. Press, London). Revised edition published 1953 as *Diamond Technology: Production Methods for Diamond and Gem Stones*.
- Groth, W., K. Beyerle, H. H. Ihle, A. Murrenhoff, E. Nann, and K. H. Welge, 1958, "Enrichment of uranium isotopes by the method of gas centrifugation," Research Report No. 510 of the Ministry of Industry and Commerce, West German publishers, Cologne-Opladen, AEC translation No. 3412.
- Gunter, E. J., Jr., 1966, "Dynamic stability of rotor-bearing systems," Scientific and Technical Information Division, Office of Technology Utilization, National Aeronautics and Space Administration, Washington, D.C., USA.
- Hertz, H., 1896, *Miscellaneous Papers* (Macmillan, New York).
- Holweck, F., 1923, "Helicoidal molecular pump," *C. R. Acad. Sci.* **177**, 43.
- Jeffcott, H. H., 1919, "The lateral vibration of loaded shafts in the neighbourhood of a whirling speed—the effect of want of balance," *Philos. Mag. Series 6*, **37**, 304.
- Jung, I., 1957, "De Laval Memorial Lecture 1957" (Swedish De Laval Steam Turbine Co., Stockholm, Sweden).
- Juvinall, R. C., 1967, *Engineering Considerations of Stress, Strain, and Strength* (McGraw-Hill, New York).
- Kauzlarich, J. J., R. W. Wavrik, and J. A. Friedericy, 1968, "Spherical pivot bearing theory," *Lubr. Eng.* **24**, Part I, 20.
- Kelley, R. E., 1963, "Rigid rotor dynamics," University of Virginia Report EP. 3912-107-63U.
- Kennard, E. H., 1938, *Kinetic Theory of Gases with an Introduction to Statistical Mechanics* (McGraw-Hill, New York).
- Kirk, R. G., and E. Gunter, 1972, "Effect of support flexibility and damping on the dynamic response of a single mass flexible rotor in elastic bearings," University of Virginia Report NASA-CR-2083.
- Maxwell, J. Clerk, 1853, "On the equilibrium of elastic solids," *Trans. R. Soc. Edinburgh* **20** Part 1, 111. Also in *Scientific Papers of Maxwell* **1**, 61.
- Maxwell, J. Clerk, 1856, in "The Origins of Clerk Maxwell's Electric Ideas, as Described in Familiar Letters to W. Thomson," communicated by Sir J. Larmor, 1936, *Proc. Cambridge Philos. Soc.* **32**, 726.
- Maxwell, J. Clerk, 1881, *A Treatise on Electricity and Magnetism*, Vols. I and II (Clarendon, Oxford). Recent edition edited by J. J. Thomson (Constable and Co., London, and Dover, New York, 1954).
- Miller, D. F., 1954, "Forced vibration of a uniform beam on damped, flexible end supports," Westinghouse Research Report R-94454-3-J.
- Milligan, J. W., and S. S. Green, 1953, "Magnetic Suspension," US Patent 2,869,935.
- Ormondroyd, J., and J. P. Den Hartog, 1928, "The theory of the dynamic vibration absorber," *Trans. Am. Soc. Mech. Eng.* **50**, A9.
- Pan, C. H. T., 1962, "Gas lubricated spherical bearings,"

- Mechanical Technology Inc. Report MT1-62TR5.
- Pinkus, O., and B. Sternlicht, 1961, *Theory of Hydrodynamic Lubrication* (McGraw-Hill, New York).
- Rayleigh, R. J. S., baron, 1877, *The Theory of Sound* (MacMillan, London). American edition with a historical introduction by Robert Bruce Lindsay (Dover, New York, 1945).
- Reynolds, O., 1886, "The theory of lubrication and its application to Mr. Beauchamp Tower's experiments, including an experimental determination of the viscosity of olive oil," *Philos. Trans. R. Soc. London* 177, Part I, 157; in *Theory of Hydrodynamic Lubrication* by O. Pinkus and B. Sternlicht (McGraw-Hill, New York, 1961).
- Rotor, H. C., 1941, *Electromagnetic Devices* (Wiley, New York/London).
- Sauer, F. M., and G. F. Garland, 1949, "Performance of the viscously damped vibration absorber applied to systems having frequency square excitation," *Trans. Am. Soc. Mech. Eng.*, published in *J. Appl. Mech.* 71, A109.
- Schlichting, H., 1968, *Boundary Layer Theory*, 6th ed. (McGraw-Hill, New York).
- Siegbahn, S., 1940. See Von Friesen, 1940, who describes Siegbahn's design for a high-speed molecular pump.
- Shaw, M. C., and C. D. Strang, 1948, "The hydrosphere—a new hydrodynamic bearing," *Trans. Am. Soc. Mech. Eng.*, published in *J. Appl. Mech.* 70, A-137.
- Shaw, M. C., and E. F. Macks, 1949, *Analysis and Lubrication of Bearings* (McGraw-Hill, New York).
- Shotter, G. F., and G. F. Tagg, 1960, *Induction Type Integrating Meters* (Pitman, London).
- Sickafus, E. N., R. B. Nelson, and R. A. Lowry, 1961, "The Holweck type molecular pump," University of Virginia Report No. EP. 4422-178-61U.
- Smith, J., 1896, described in "De Laval Memorial Lecture 1957" by I. Jung (Swedish De Laval Steam Turbine Co., Stockholm).
- Sommerfeld, A., 1904, "The hydrodynamic theory of lubrication," *Z. Angew. Math. Phys.* 50, 97.
- Steenbeck, M., G. Zippe, and R. Scheffel, 1957, "Schnellaufende Gaszentrifuge," German Patent 1.071.593 dated 14.11.57.
- Stott, V., 1931, "Investigation of problems relating to the use of pivots and jewels in instruments and meters," *Collected Researches of the National Physical Laboratory* (HMSO, London), Vol. 24, Paper 1, p. 1.
- Taylor, G. I., 1923, "Stability of a viscous liquid contained between two rotating cylinders," *Philos. Trans. R. Soc. London*, Ser. A 223, 289.
- Timoshenko, S. P., 1928, *Vibration Problems in Engineering* (Van Nostrand, Princeton/New York). Third edition 1955.
- Timoshenko, S. P., 1953, *History of Strength of Materials* (McGraw-Hill, New York).
- Towers, B., 1883, "First report on friction experiments," *Proc. Inst. Mech. Eng. London* 34, 632.
- Von Friesen, S., 1940, "Large molecular pumps of the disk type," *Rev. Sci. Instrum.* 11, 362.
- Watts, P., 1883, "On a method of reducing the rolling of ships at sea," *Trans. Inst. Naval Archit.* 24, 165.
- Whipple, R. T. P., 1951, "Theory of the spiral grooved thrust bearing with liquid or gas lubricant," UK Atomic Energy Authority Report AERE-T/R-622.
- Whitley, S., 1967, "The design of the spiral groove thrust bearing," Paper No. 13, *Third Gas Bearing Symposium on Design Methods and Applications* (Department of Mechanical Engineering, University of Southampton, England).
- Whitley, S., 1979, "The uranium ultracentrifuge," *Phys. Technol.* 10, 26.
- Wood, A., 1940, *Acoustics* (Blackie & Son, London/Glasgow).
- Zippe, G., 1960, "The development of short bowl ultracentrifuges," US Atomic Energy Commission Report ORO-315, University of Virginia Report EP-4420-60 U.